nature protocols

PROTOCOL

https://doi.org/10.1038/s41596-021-00548-8

Check for updates

Whole-brain functional ultrasound imaging in awake head-fixed mice

Clément Brunner[1,2,3,4,9], Micheline Grillet[1,2,3,4,9], Alan Urban[1,2,3,4], Botond Roska[5,6,7], Gabriel Montaldo[1,2,3,4,10]✉ and Emilie Macé[8,10]✉

Most brain functions engage a network of distributed regions. Full investigation of these functions thus requires assessment of whole brains; however, whole-brain functional imaging of behaving animals remains challenging. This protocol describes how to follow brain-wide activity in awake head-fixed mice using functional ultrasound imaging, a method that tracks cerebral blood volume dynamics. We describe how to set up a functional ultrasound imaging system with a provided acquisition software (miniScan), establish a chronic cranial window (timing surgery: ~3–4 h) and image brain-wide activity associated with a stimulus at high resolution (100 × 110 × 300 μm and 10 Hz per brain slice, which takes ~45 min per imaging session). We include codes that enable data to be registered to a reference atlas, production of 3D activity maps, extraction of the activity traces of ~250 brain regions and, finally, combination of data from multiple sessions (timing analysis averages ~2 h). This protocol enables neuroscientists to observe global brain processes in mice.

Introduction

Systems neuroscience aims to understand the circuits and computations underlying brain functions and behaviors. However, one major challenge for systems neuroscience is that circuits span multiple spatial and temporal scales, from the level of the synapse to the entire brain. In past decades, mice emerged as a popular model for systems neuroscience because of the variety of genetic and probing tools available to interrogate local neuronal circuits. Neuroscientists can now target, manipulate and record specific neuronal populations in the context of behavior in mice[1–3]. Despite these advances, there is a limited number of options for capturing whole-brain activity, particularly under awake conditions. Large-scale imaging techniques exist but have specific limitations, such as depth of field, brain coverage, resolution or compatibility with behavior (see 'Comparison with other methods'). Difficulty imaging at the whole-brain scale introduces a bias toward investigating a handful of regions at a time, resulting in important whole-brain aspects of the function studied potentially being omitted.

Functional ultrasound imaging (fUS)[4] is an emerging technology that has the potential to fill this gap in the context of mouse research. fUS reports relative changes in cerebral blood volume (CBV) as a proxy for neuronal activity[5] and offers a set of unique features and advantages. First, ultrasound penetrates deep into tissue: a ~15 MHz ultrasound frequency produces images with ~1 cm penetration, ideal for imaging the entire depth of the mouse brain. Second, fUS offers a high spatio-temporal resolution (100 × 110 × 300 μm, 10 Hz), which enables the dynamics of brain activity to be captured through the CBV signal. Finally, the portability of the ultrasound scanner and the compact size of the probe used for fUS make it easy to combine with other methods and to integrate into routine neuroscience experiments.

Nonetheless, adapting fUS to chronic imaging of whole-brain activity in awake mice presents specific challenges. First, because ultrasound is strongly attenuated by the skull, a cranial window must be implanted. Second, because ultrasound high-resolution probes are limited to a single brain slice, the imaging procedure must integrate technical constraints (how to scan the brain efficiently) with constraints linked to the task in which the mouse is engaged. Finally, it is necessary to have an

[1]Neuro-Electronics Research Flanders, Leuven, Belgium. [2]VIB, Leuven, Belgium. [3]Imec, Leuven, Belgium. [4]Department of Neurosciences, KU Leuven, Leuven, Belgium. [5]Institute of Molecular and Clinical Ophthalmology Basel, Basel, Switzerland. [6]University of Basel, Basel, Switzerland. [7]NCCR Molecular Systems Engineering, Basel, Switzerland. [8]Brain-Wide Circuits for Behavior Lab, Max Planck Institute of Neurobiology, Martinsried, Germany. [9]These authors contributed equally: Clément Brunner, Micheline Grillet. [10]These authors jointly supervised this work: Gabriel Montaldo, Emilie Macé. ✉e-mail: gabriel.montaldo@nerf.be; emace@neuro.mpg.de

understanding of how to analyze the data, how to combine data from different imaging sessions and how to localize brain structures in this new type of image.

We recently published a study in which we successfully overcame these challenges[6]. We used fUS to reveal all the brain regions activated in the mouse brain during a visuomotor reflex, and how these regions are functionally affected during various perturbations of the reflex. This protocol facilitates application of fUS and provides neuroscientists with a standard approach for capturing in an unbiased way the whole-brain activity elicited by a behavior or brain function in head-fixed mice. It outlines how to set up an fUS experiment and provides a standard pipeline for data acquisition and statistical analysis. We believe that this protocol is essential to facilitate comparisons across laboratories, and for this method to be widely adopted in systems neuroscience.

Development of the protocol

fUS is a versatile method that has been implemented in different animal models. To date, fUS has been successfully used in rats[7–10], birds[11], rabbits[12], ferrets[13] and nonhuman primates[14,15]. fUS has also been used for intraoperative functional neurosurgery in adult humans[16,17] and for transfontanelar neuromonitoring in neonates[18]. On the technological front, the development of miniature probes has broadened the applications of fUS to image rodents under freely moving conditions[8,19]. More recently, the development of matrix probes allowed for volumetric imaging (vfUSI), although at a reduced spatial resolution[20,21]. In addition to being applicable to a wide range of species and the various technical possibilities, fUS has also been successfully applied in different fields of neuroscience, from fundamental neuroscience, to preclinical research[9,10,22] and in the clinic[16,17].

The surgical protocol, imaging parameters, data processing and behavioral context have evolved since we published our first study using rodents 10 years ago[4]. This has resulted in various experimental procedures being used, with differing procedures being optimal depending on the application. Based on our extensive experience of both the challenges and the most up-to-date capabilities of the method, we provide here a comprehensive protocol to set up the equipment and software, perform the surgery, image the brain and process the data. Until our recent publication that outlined a general unbiased whole-brain approach[6], experiments were targeted at a specific part of the brain to answer a specific question. We now present a detailed procedure that can be used to obtain a whole-brain view of the activity evoked by a stimulus or event. We provide standardized analysis outputs to ensure that different animals or sessions can be compared. Finally, we explain how to conduct these experiments in awake head-fixed mice, a context that hopefully suits the needs of many neuroscientists.

Applications

The main use of this protocol we envisage is to identify the brain-wide networks activated by an 'event' and to extract the time course of activity in these regions. Here we give the specific example of a visual stimulus, but this can conceptually be replaced by any other sensory stimuli, a cued task or any other triggered behavioral event without changing the procedure.

In its current form, particularly the analysis, the protocol is primarily designed for events that can be repeated multiple times. Localizing the network of regions active during an event, and determining how this network is dynamically engaged in the event, can provide valuable information to understand the large-scale interactions involved in the underlying neural processes. The ability to image whole-brain activity in awake mice, and repeatedly for months, allows for a large repertoire of tasks or events to be studied with fUS. For example, it is possible to follow the engagement of the whole brain across the learning of a task, test the effect of a drug over time or study the effect of progression of a disease on brain activity.

One key asset of this protocol is its compatibility with other technologies. Combining fUS with electrophysiology[4,6,7] is important for confirming activation at the neuronal level in deep brain regions, or for identifying the role of specific neuronal populations in the activity detected. The combination of fUS with optogenetic control of genetically defined neuronal populations can help identify cell-type-specific connectivity across the entire brain, and also be used to examine the behavioral consequences of manipulating targeted populations[21,23]. While it is beyond the scope of this protocol to provide examples for all combinations with other methods, this protocol should serve as a starting point for conducting such experiments. In the case of electrophysiology and optogenetics, the main modification would consist of implanting an electrode or an optical fiber during the cranial window surgery in a position that allows space for positioning the ultrasound probe during the imaging session. For optogenetics, viral vectors can also easily be injected into the brain during

the same surgical preparation, the sensory stimulus is replaced by light stimulation and the data analysis is conceptually the same. Using a chronic window for fUS is also compatible with wide-field[24–27] or two-photon calcium imaging[28,29], therefore extending the range of its application.

Comparison with other methods

Large-scale methods are commonly used for mouse brain imaging, but suffer from specific limitations. For example, functional magnetic resonance imaging (fMRI) can capture whole-brain activity via hemodynamic responses (BOLD-fMRI, CBV-fMRI) in a noninvasive way, but remains mostly limited to anesthetized animals. While challenging, awake fMRI strategies are emerging[30,31]; nonetheless, intrinsic MRI scanner specifications strongly limit the repertoire of behaviors that are compatible with fMRI. Moreover, an MRI scanner is a considerable investment that is not available to all laboratories. Wide-field calcium imaging is widely used by neuroscientists to efficiently capture neuronal activity of genetically defined populations of neurons on a large scale, and with good spatiotemporal resolution during behavior, but remains mostly limited to the dorsal part of the cortex[32]. The recent development of the neuropixels probe[33] for electrophysiology now allows thousands of neurons from multiple brain regions of awake behaving rodents to be recorded[34]. However, the brain coverage is intrinsically limited given that the location of the probe determines which regions can be recorded and because only a few of these probes can be implanted simultaneously. Finally, multifiber photometry simultaneously targets cortical and subcortical regions of the mouse brain[35], but it remains constrained to tens of recording sites.

Beyond the established methods discussed above, recent developments have also shown the potential of combining different modalities. For example, the combination of wide-field calcium imaging and fMRI[36] gives access to neuronal activity in the cortex while benefiting from the whole-brain view offered by fMRI. Similarly, whole-brain optoacoustic imaging of neuronal activity is promising as it allows detection of the signal from genetically encoded calcium indicators even deep in the brain[37]. However, both these approaches are still limited to anesthetized mice to date. Therefore, compared with other methods, fUS is a practical way to assess the brain-wide activity associated with a stimulus or an 'event' in awake head-fixed mice.

In terms of affordability, the ultrafast ultrasound scanner used in this protocol currently costs ~€100,000 (excluding the high-performance computing workstation required to enable extended acquisition and processing capabilities) and the probe costs ~€7,000. Therefore, the acquisition of a functional ultrasound system is in the same price range as a commercial two-photon microscope, but one order of magnitude cheaper than a small-animal MRI scanner. While this is a considerable investment that is not available to all laboratories, the fUS system does have the advantage of not requiring additional maintenance costs.

Limitations

One practical limitation of this protocol is that only one cross-section of the brain can be imaged by the linear ultrasound probe; therefore, it must be motorized to scan the brain volume. The scanning approach takes time and requires repetitions of the stimulus or 'event' studied. Repetition can lead to adaptation, and should be partially mitigated by choosing an appropriate intertrial interval or time between imaging sessions. As mentioned before, the development of matrix ultrasound probes will likely alleviate this limitation in the future[21]. However, volumetric imaging (vfUSI) is technologically challenging, and the resolution is currently limited to ~300 μm^3. Note that the surgical and data analysis steps presented in this protocol are nonetheless directly applicable to vfUSI.

A second practical limitation of this protocol is motion artifacts. Filtering strategies—namely high-pass and singular value decomposition (SVD) filters[38]—can manage tissue motion induced by breathing or small movements, but fail for strong and sudden motion. Head-fixed mice can move during the imaging sessions, and abrupt movements induce noise in the fUS data. To date, the signal from the noisy frames cannot be recovered, and the corresponding frames are lost and must be discarded from the analysis. Nevertheless, as presented in this protocol, the animal's careful habituation to the setup and head fixation is sufficient to drastically reduce the proportion of rejected frames to below 10%, which corresponds to our tolerance rating.

Some limitations are more general to imaging techniques requiring a chronic cranial window and head fixation, such as wide-field calcium imaging[25,39]. Although invasive, a cranial window is crucial to achieve high-quality imaging with fUS. An alternative strategy is thinning the skull[7,10], but bone regrowth usually degrades imaging quality for deep brain structures over time, making this approach

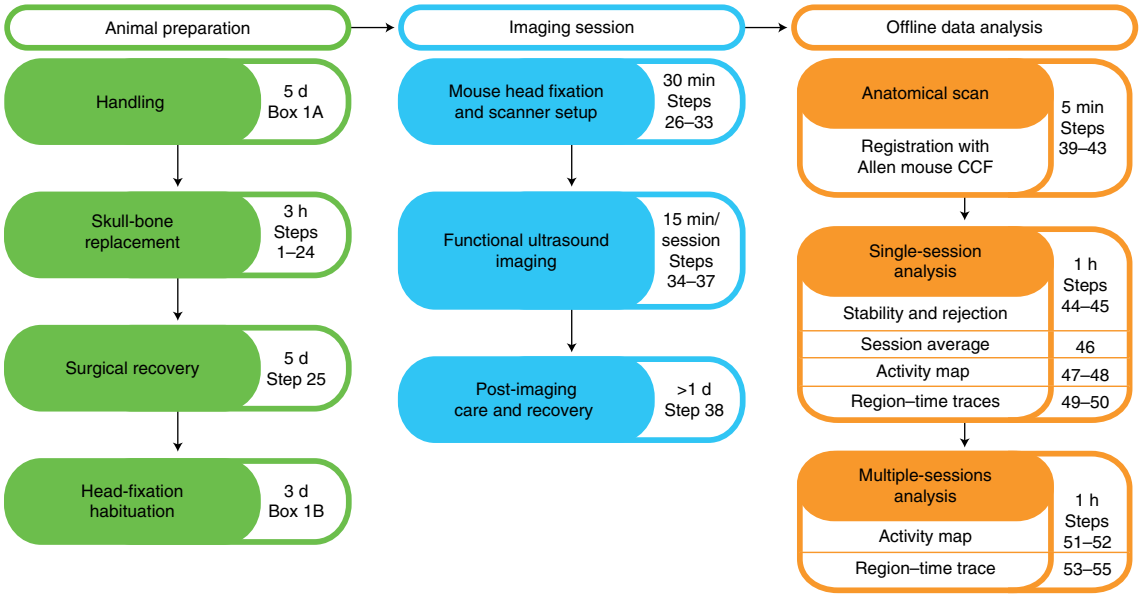

Fig. 1 | Flowchart of the procedure. Description of the three main stages encountered during chronic fUS of brain-wide activity in awake head-fixed mice. Animal preparation (green boxes), imaging session (blue boxes) and offline data analysis (orange boxes) protocol described in the Procedure. Timing and numbers refer to corresponding steps of the Procedure. CCF, Common Coordinate Framework, v3.

challenging for longitudinal imaging. Head fixation also adds constraints to the repertoire of behaviors that can be explored, and it can stress the animal. Freely moving imaging with fUS is possible but with a reduced field of view. This approach is not yet sufficiently developed to replace head fixation when looking at whole-brain activity[8,19].

Finally, this protocol using fUS monitors the vascular signal as a proxy of neuronal activity. Unlike two-photon or wide-field calcium imaging, fUS cannot follow the activity of individual cells or of genetically defined cell types. fUS depends on neurovascular coupling, which may vary across brain regions or across experimental conditions. The possible effects of neurovascular coupling on imaging results have been reviewed previously[40]. However, the compatibility of this protocol with other tools such as electrophysiology offers the opportunity to verify the whole-brain results locally at the neuronal level.

Overview of the procedure

The procedure describes how to undertake chronic brain-wide fUS in head-fixed mice. The entire workflow is shown in Fig. 1. The procedure was optimized on adult mice (>8 weeks) and can be performed similarly on both male and female. Sex is an important biological variable that should be taken into consideration; therefore we recommend to use mice from both sexes whenever possible.

The first part of the procedure describes how to prepare the animal. fUS requires a cranial window to be in place as the skull strongly attenuates ultrasound; thus establishment of a chronic cranial window that gives access to a large fraction of the brain volume is a critical step of the protocol. We also provide photos and diagrams to facilitate preparation of such a window (Fig. 2). It is important to handle the mouse appropriately and habituate it to the imaging setup prior to imaging. Habituation reduces the stress of the mouse caused by head fixation or new environments, and thus limits strong motion artifacts and improves the reproducibility of the results (Box 1). Although animal habituation helps to reduce variability, we recommend that behavior is always monitored using body and facial cameras whenever possible. Because of this variability, it is beneficial to combine a large number of sessions per and across mice to obtain a strong statistical result.

The second part of the protocol outlines how to run an imaging session. This includes how to set up an fUS system, design the experiment, acquire data and handle the animal during the imaging session (Fig. 3). We describe the hardware requirements, but more importantly, we offer a custom-made graphical user interface to assist data acquisition and synchronization of the ultrasound system with the motor, which is essential for scanning the brain. The exact design of the experiment (e.g., stimuli and number of brain slices) depends on the application. Here, we provide a detailed example for acquiring the whole-brain activity elicited by a 1 s short visual stimulus.

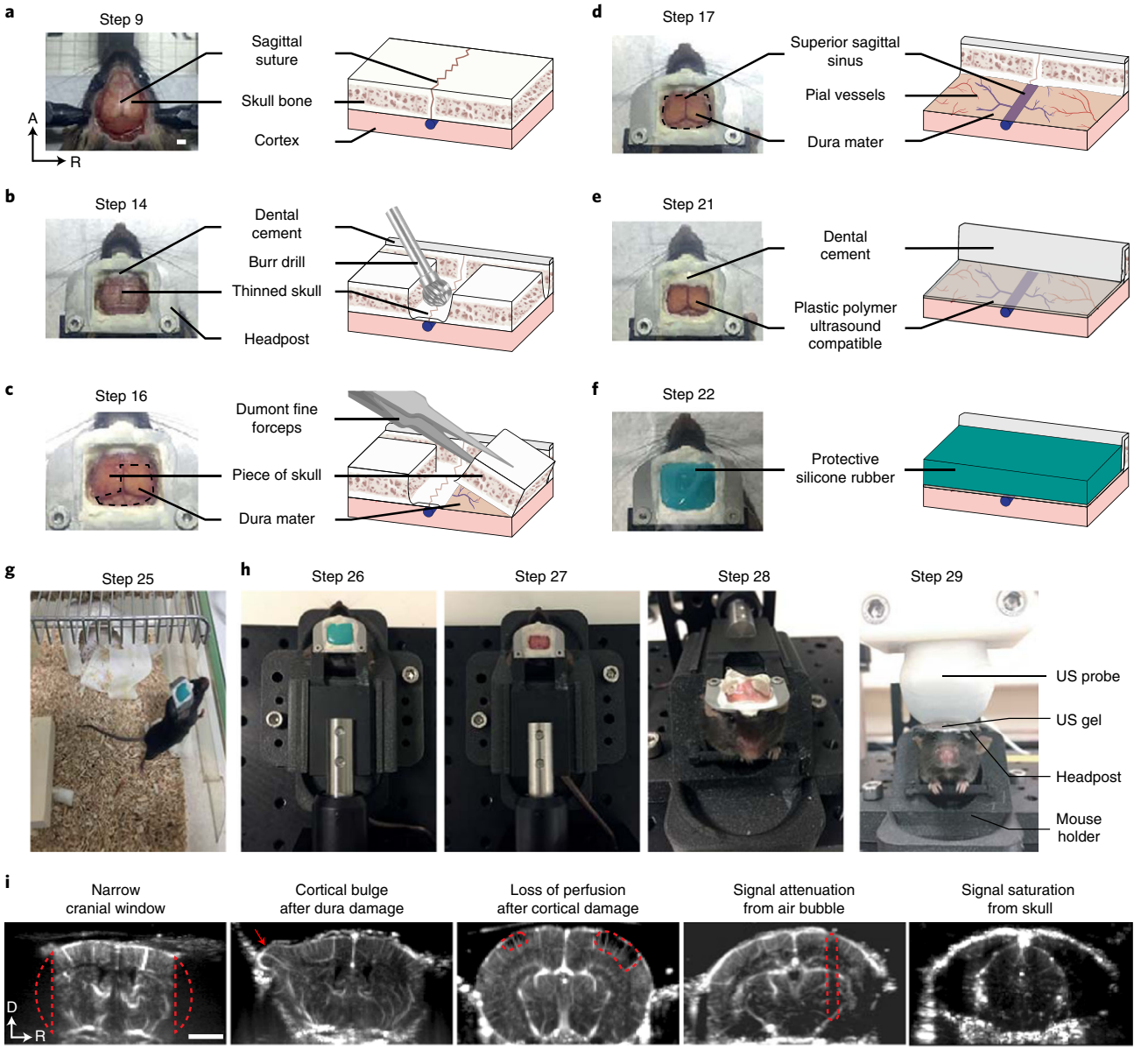

Fig. 2 | Surgical procedure for chronic whole-brain imaging of awake head-fixed mice. a–f, Pictures and detailed illustrations of the surgical procedure for headpost cementing, cranial window and bone replacement. Step 9: the skin and periosteum are removed, temporal muscles retracted and skull bone cleaned (**a**). Step 14: the headpost is cemented to the skull. Squares of skull are thinned with a hand drill (**b**). Steps 16–17: the cranial window is progressively opened by gently removing the square skull plaques with fine forceps (dotted black region). The dura mater and the surface of the brain remain intact (**c**,**d**). Step 21: the cranial window is covered with a 50 µm plastic sheet (polymethylpentene, plastic polymer ultrasound compatible) cemented to the headpost (**e**). Step 22: apply the silicone rubber over the plastic cover to protect the preparation and ease access for imaging (**f**). Step 25: picture of the mouse in its homecage before imaging session (**g**). Steps 26–29 from left to right: pictures of the mouse preparation for the imaging session from head-fixation, removal of the silicone plug, ultrasound gel application and adjustment of the probe over the brain window. US, ultrasound (**h**). Examples of problematic µDoppler images (from left to right) due to signal attenuation from a narrow cranial window (red dotted areas), surgical damage provoking a bulge (red arrow) or some cortical damage (red dotted areas). Signal attenuation caused by an air bubble (red dotted area) trapped in the ultrasound gel; and signal saturation from the skull (**i**). Troubleshooting guidance can be found in Table 1. A, anterior; R, right; D, dorsal; R, right. Scale bars, 2 mm. All animal experiments were approved and conducted according to the Committee on Animal Care of the Catholic University of Leuven, Belgium, the Veterinary Department of the Canton of Basel-Stadt, Switzerland, and European guidelines.

The third part of the protocol discusses the data analysis. We supply software for the complete analysis of fUS data (Figs. 4 and 5; Supplementary Software (also available at https://github.com/nerf-common/whole-brain-fUS)). Registration and segmentation processes are particularly important for comparing datasets across sessions, animals and conditions, as for other whole-brain methods such as fMRI[41,42]. The software includes a graphical user interface to assist with the registration of the ultrasound data on a reference atlas: the Allen Mouse Common Coordinate Framework (CCF)[43].

Box 1 | Mouse handling and head-fixed habituation ● Timing ~1 h

Presurgery handling and postsurgery habituation are time-consuming but dramatically reduce animal anxiety and consequently increase both the quality and the repeatability of the acquisition.

(A) Presurgery mouse handling
Five days before surgery, handle mice daily following behavioral expert recommendations as described in refs. [47,48]. We progressively habituate mice to be nonaversively hand-cupped, and, once accustomed to the experimenter (e.g., exhibiting grooming behaviors while hand-cupped), mice are progressively acclimatized to walking through the body tube of the experimental fUS setup.

(B) Postsurgery head-fixation habituation
Once they have recovered from the surgical procedure (Step 25 of the Procedure), mice should be daily habituated to head fixation[49] after walking through the body tube. Fixation periods should be progressively increased, from 10 min the first day up to 1 h after 3 d. In the case of signs of discomfort, such as excessive movement and/or vocalization, the experimenter should stop the head-fixation session.

We also present a method for creating region-specific activity curves, based on a standardized list of ~250 regions from the Allen Mouse CCF (Fig. 6). Finally, we detail how to produce voxel-based and region-based activity maps in response to a given stimulus, and present examples in the case of the visual stimulation (Fig. 6). The outputs of this protocol (whole-brain activity maps) are given with a statistical threshold, which assesses the significance of the stimulus-induced increase or decrease of activity compared with baseline periods. As such, there is generally no need for a specific control group of animals.

Materials

Animals

- Wild-type mice (we used 8-week-old C57BL/6 mice; Janvier Labs; the results presented here are from male mice, but this protocol can be used with both males and females) **! CAUTION** Any experiments involving live mice must conform to institutional guidelines, and local and national regulations. All experiments presented in this protocol were approved by the Committee on Animal Care of the Catholic University of Leuven, Belgium, and the Veterinary Department of the Canton of Basel-Stadt, Switzerland, and were in accordance with standard ethical guidelines (European Communities Guidelines on the Care and Use of Laboratory Animals, 86/609/EEC). All efforts were made to minimize the number of animals used.

Reagents

Drugs

! CAUTION All drugs listed are controlled substances and must be used according to institutional and governmental guidelines.

- Isoflurane 1000 mg/g (Iso-Vet, Dechra, cat. no. 2909737) **! CAUTION** Isoflurane is an anesthetic gas with known adverse effects in humans and therefore must be handled in accordance with institutional guidelines. Isoflurane should only be used in a designated area with appropriate ventilation and a charcoal-based scavenging system. Isoflurane is suspected to reduce fertility and harm an unborn child. Pregnant or breastfeeding personnel should avoid exposure to it.
- Fentanyl 0.05 mg/ml (Curamed, cat. no. GTIN 7680534840018)
- Medetomidine 1 mg/ml (Domitor, Orion Pharma, cat. no. 1070499)
- Midazolam 5 mg/ml (Ratiopharm, cat. no. PZN-04921530)
- Ketamine 100 mg/ml (Nimatek, Dechra, cat. no. 3120060)
- Atipamezole 5 mg/ml (Revertor, Vibrac, cat. no. GTIN 04042668304324)
- Flumazenil 0.1 mg/ml (Sintetica, cat. no. GTIN 7680594000018)
- Naloxone 0.4 mg/ml (Orpha, cat. no. GTIN 7680569520015)
- Buprenorphine 0.3 mg/ml (Vetergesic, Ecuphar, cat. no. 263627)
- Dexamethasone 2 mg/ml (Rapidexon, Dechra, cat. no. 1421825)
- Emdotrim 10% sol (Ecuphar, cat. no. 1633163)
- Cefazolin 1 g (Sandoz, cat. no. 1676691)
- Enrofloxacin 22.7 mg/ml (Bayer Healthcare, cat. no. 08713254)

Reagents for surgical procedure

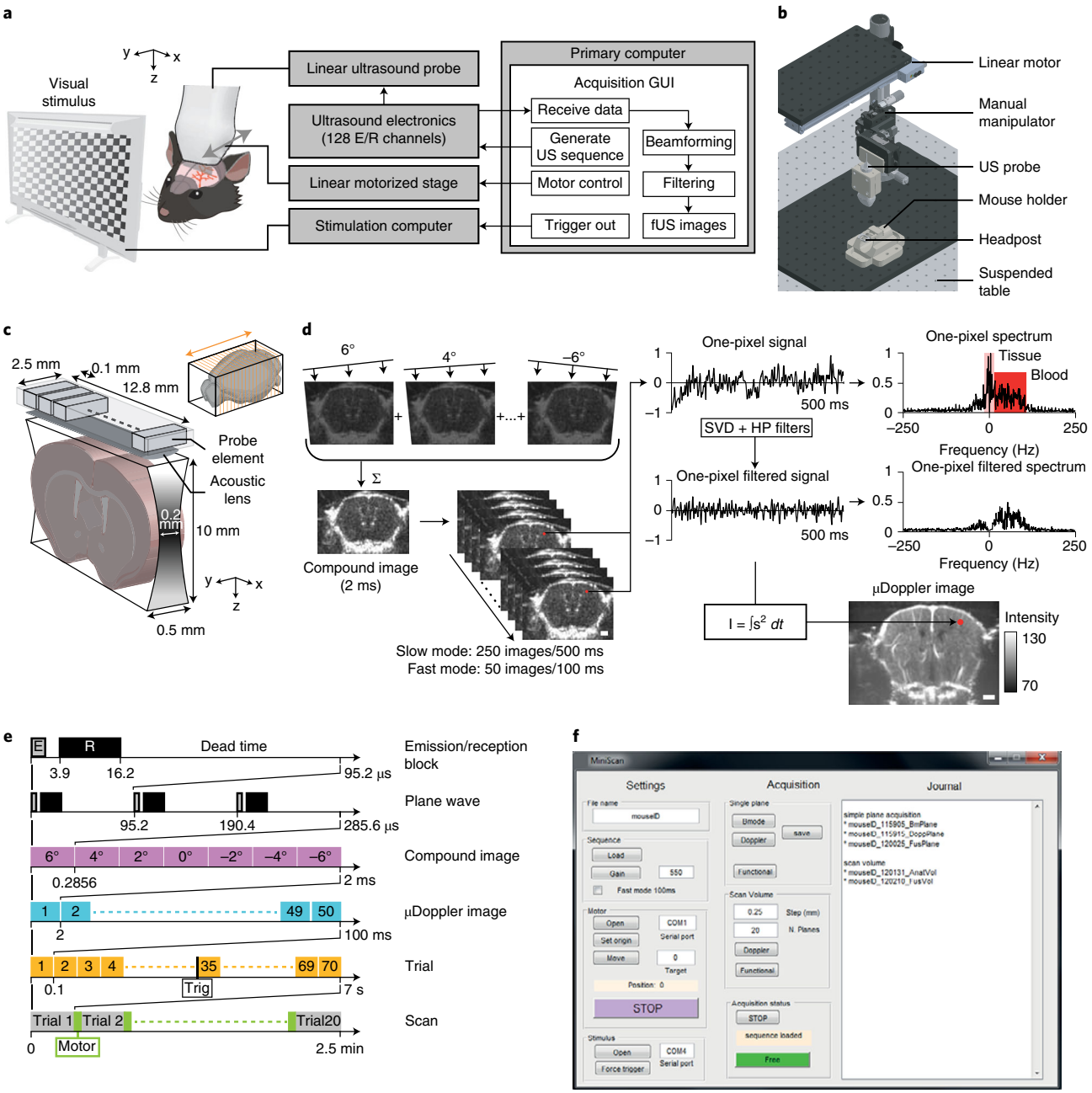

Fig. 3 | Real-time whole-brain fUS of stimulus-evoked activity. a, Connectivity diagram of the fUS setup, illustrating the computers, hardware and software required to perform real-time whole-brain imaging. The acquisition GUI generates the ultrasound sequence, receives the data acquired via the ultrasound electronics and the ultrasound probe, and then beamforms, filters and processes the dataset to produce μDoppler fUS images in real time. The GUI also controls the linear motorized stage, and the stimulation computer to move the ultrasound probe and trigger the visual stimulus, respectively. Required tools and equipment are listed in 'Equipment' and the manual of the Supplementary Software. **b**, CAD schematic of the experimental setup for performing whole-brain fUS in awake head-fixed mice (see Supplementary Data). **c**, Schematic representation of the dimensions of the linear ultrasound probe and of a single coronal plane acquired using this probe. Top right: schematic of a whole-brain scan by moving the probe along the antero-posterior axis. **d**, Diagram of the steps required to generate a single μDoppler image. Seven tilted plane waves are transmitted in 2 ms to build one compound image, and 250 compound images are accumulated in 500 ms (or 50 images in 100 ms for the fast mode), coherently added, decomposed into frequencies by a fast Fourier transform, filtered with high-pass and SVD filters to finally extract the intensity I of the signal and then generate a μDoppler image. Plots presented here are one-pixel signals. Scale bar, 1 mm. **e**, Timeline of the experimental sequence from ultrasound emission/reception block to functional scan. Box 2 provides a detailed description of the experimental sequence. **f**, Screenshot of the miniScan software for acquisition of functional ultrasound images. The 'Settings' panel (left) allows the user to log the experiment, load the imaging sequence, set motor parameters and control the slave computer to trigger the visual stimulus. The 'Acquisition' panel allows the user to generate individual Bmode and μDoppler images, perform functional scans and check the status of the acquisition. All experimental information, saved images and scans are logged in the 'Journal'. More details can be found in the manual of the Supplementary Software. All animal experiments were approved and conducted according to the Committee on Animal Care of the Catholic University of Leuven, Belgium, the Veterinary Department of the Canton of Basel-Stadt, Switzerland, and European guidelines.

- Iso-betadine solution (Meda, cat. no 82-217)
- Lubricant eye gel (Duratears, Novartis Pharma, cat. no. RVG 10187)
- Bone wax (CP Medical, cat. no. CPB31A)
- Ethanol 70% (VWR, cat. no. 83805) **! CAUTION** Ethanol solution is highly volatile and flammable. Careful handling is recommended.

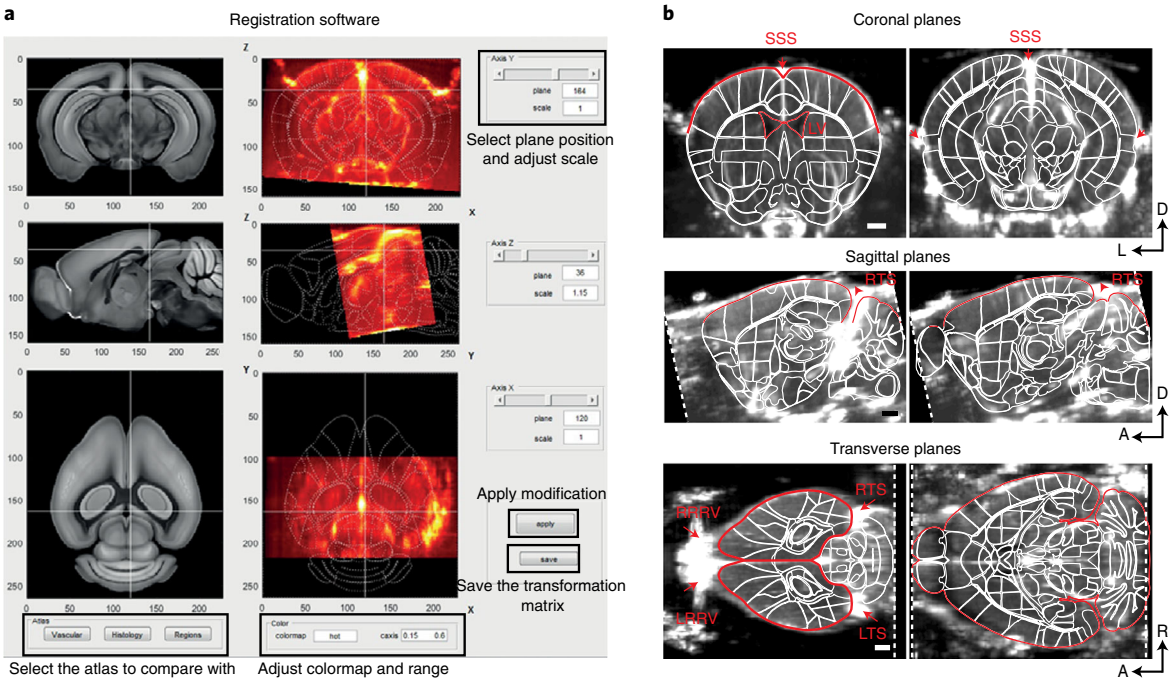

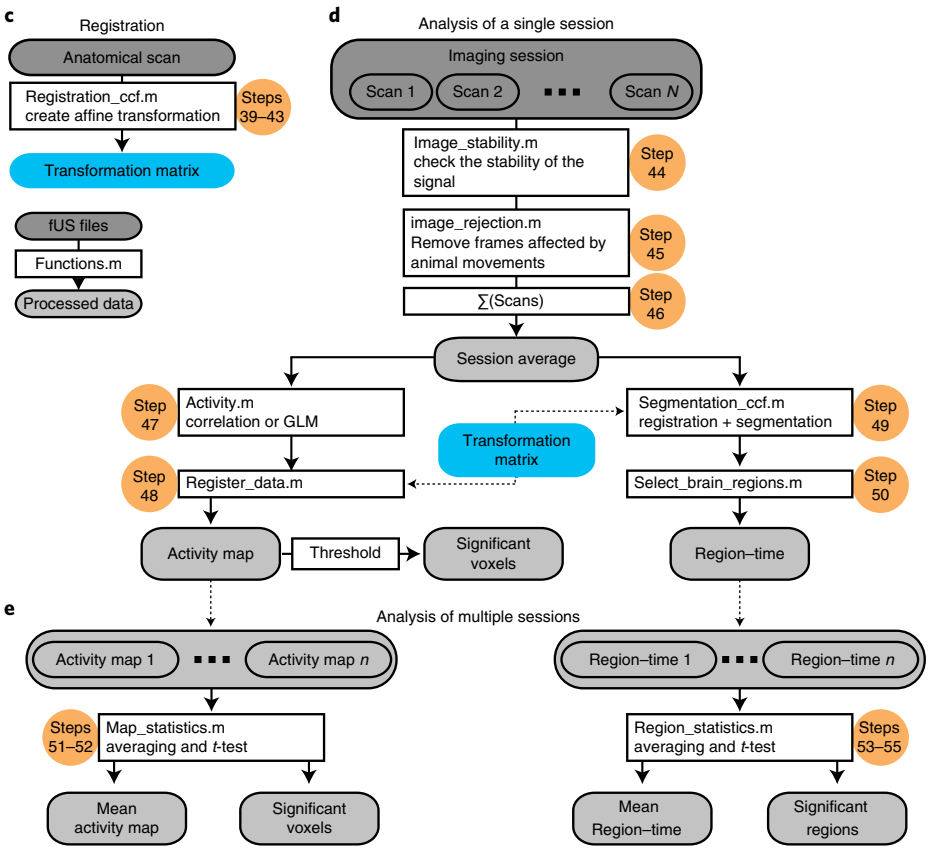

- Glucose (Sigma-Aldrich, cat. no. G7021)
- Vetbond tissue adhesive (3M, cat. no. 70200742529)
- Resin cement kit, including catalyst V, monomer, polymer L-type radiopaque, red activator, adjustable precision applicator brushes and sponge spear (Sun Medical Co., Ltd, cat. no. Super-Bond C&B) **! CAUTION** Resin cement is highly volatile and flammable. Avoid skin contact, and limit vapor inhalation. Careful handling is recommended.
- Polymethylpentene TPX plastic sheet, 50 μm (Goodfellow, cat. no. ME311051)
- Silicone rubber (Smooth-on, cat. no. Body Double-Fast Set)
- DietGel Recovery (ClearH2O, cat. no. 72-06-5022)
- Sterile saline (any)
- Compressed air duster (any) **! CAUTION** Compressed air bottle is highly flammable. Careful handling is recommended.

Reagents for imaging

- Sterile saline (any) or artificial cerebrospinal fluid (Diacleanshop, cat. no. LERE-S-LSG-1000-1)
- Ultrasound gel (Aquasonic Clear, Parker Laboratories, cat. no.03-08).

Equipment

Surgical setup, device and instruments

- Anesthesia system with induction chamber (TemSega, cat. no. MiniHUB V3)
- Bright-field stereomicroscope (Leica Microsystems, cat. no. A60)
- Stereotaxic frame and accessories (ear bars, nose clamp) (Stoelting, cat. no. 51600)
- Physiosuite system for temperature control (Kent Scientific, cat. no. PS-CO2-RT)
- Surgical trimmer (Stoelting Co., cat. no. 51470V)
- Scalpel handle and blades (Fine Science Tools, cat. no. 10003-12 and 10011)
- Fine straight scissors CeramaCut (Fine Science Tools, cat. no. 14958)
- Dumont fine and 45°-angled forceps (Fine Science Tools, cat. no. 11252-30 and 11251-35)
- 0.5 mm burrs (Fine Science Tools, cat. no. 19007-05)
- High-speed rotary micromotor (Foredom Electric Co., cat. no. K.1070)
- Hot bead sterilizer (Fine Science Tools, cat. no. 18000-45)
- Unmounted absorption triangles (Fine Science Tools, cat. no. 18105-03)
- Spatula (Fine Science Tools, cat. no. 10092-12)
- Sterile gel foam (any)
- Sterile 0.5 ml syringes (any)
- Sterile pipette (any)
- Sterile cotton tip applicators (any)
- Ruler and fine-point surgical marker (any)

fUS system

- Ultrasound scanner (Verasonics, cat. no. Vantage 128)
- Linear ultrasound transducer (Verasonics, cat. no. L22-14Vx or Vermon, cat. no. L15-Xtech)
- Host computer (AUTC cat. no. HPC-fUSI-2 or Verasonics, cat. no. host computer or custom computer). The miniScan demo acquisition graphic user interface (GUI) can be operated on any computer equipped with a video card (Nvidia, GTX-Series, or superior). Note that a high-performance computing workstation (AUTC, cat. no. HPC-fUSI-2) is required to enable extended acquisition and processing capabilities. This workstation includes a dual CPU (Intel Xeon), 4 GPUs (Nvidia,

◀ **Fig. 4 | Registration and processing of whole-brain fUS data. a**, Screenshot of the GUI for registering the dataset with the Allen Mouse CCF. **b**, Coronal, sagittal and transverse views of the affine transformation of the anatomical scan with the Allen Mouse CCF (white outlines). Red lines delineate edges of the brain volume; red arrows give the position of the main brain vessels. Lines and arrows provide a good template for registering the dataset and for further transformations. **c**, Registration of the anatomical scan with the Allen Mouse CCF generates a transformation matrix applied in **d**. **d**, Workflow for a single imaging session analysis with steps for noise rejection and session averaging. Two distinct paths of computing (including a registration step using the transformation matrix generated in **a**) enable either an activity map or region–time traces to be extracted. **e**, Activity maps and region–time traces from multiple sessions are averaged to test whether voxels or regions are significantly activated in response to the stimulus. Numbers refer to corresponding steps in the Procedure. A, anterior; D, dorsal; R, right; L, left; SSS, superior sagittal sinus; L/R-TS, left/right transverse sinus; L/R-RRV, left or right rostral rhinal vein. LV, lateral ventricles. Scale bars: 1 mm. All animal experiments were approved and conducted according to the Committee on Animal Care of the Catholic University of Leuven, Belgium, the Veterinary Department of the Canton of Basel-Stadt, Switzerland, and European guidelines.

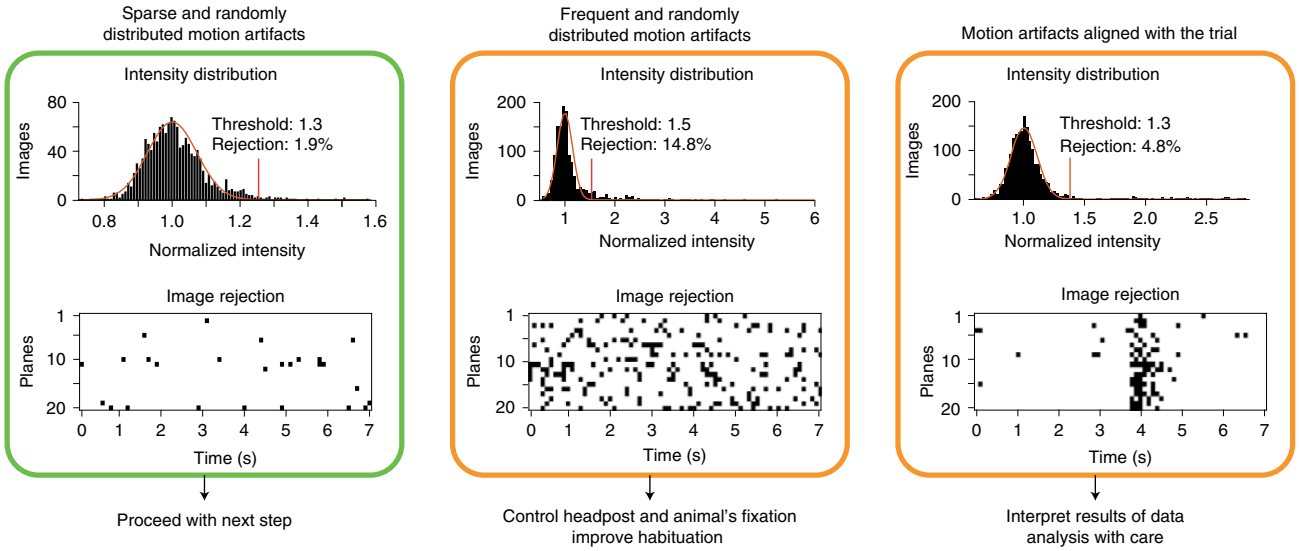

Fig. 5 | Data stability and motion artifact rejection. Detection of motion artifact and image rejection in three conditions that might be observed during fUS of awake head-fixed mice (left to right: sparse and random, frequent and random, aligned with trial) and how to proceed further for each condition. Details about threshold and image rejection can be found in Step 44 of the Procedure and in the manual of the Supplementary Software.

RTX-Series), DDR4-128 DIMM (Infineon), 1 TB SSD PCI-E NVMe (Samsung), 8 TB HDD SATA (Western Digital)

Visual stimulation

- Stimulus computer (DELL, cat. no. Optiplex)
- 27″ LCD monitor (Iiyama, cat. no. ProLite XB2783HSU)
- USB-RS232 converter (StarTech, cat. no. ICUSB232V2)

fUS platform

- Antivibration air-suspended table (TMC, cat. no. 63-500)
- Manual micromanipulator (Marzhauser Wetzlar, cat. no. MM33)
- Motorized-linear stage (Zaber Technologies, cat. no. T-LSM200A)
- Ultra-low head cap screws (Misumi, cat. no. CBSTSR2-3) and driver (iFixit, cat. no. IF145-299-4)
- CAD file of the stainless-steel headpost, see Supplementary Data, laser-cut in a 1 mm thick stainless-steel sheet (200 × 200 mm; Salomon's Metalen B.V., cat. no. Roestvrijstaal T-430)
- CAD file of the mouse holder, for 3D printing, see Supplementary Data
- CAD of the probe holder, for 3D printing, see Supplementary Data
- CAD experimental setup, see Supplementary Data

Software

- Microsoft Win10 Pro 64 bits
- MATLAB (MathWorks, https://www.mathworks.com/products/matlab.html)
- CUDA toolkit (https://developer.nvidia.com/cuda-downloads)
- PsychoPy2 (http://www.psychopy.org)
- MiniScan, a custom-written MATLAB acquisition software, see Supplementary Software. See Github repository for potential updates (https://github.com/nerf-common/whole-brain-fUS)[44]
- Custom-written MATLAB analysis codes, see Supplementary Software. See Github repository for potential updates (https://github.com/nerf-common/whole-brain-fUS)[44]

Example dataset

The dataset analyzed in this protocol is freely available on Zenodo[45] and analyzed following the scripts in Supplementary Software (see Github/Zenodo repository for potential updates[44]). Follow the instructions provided in the manual of the Supplementary Software to analyze the dataset as shown in Fig. 6.

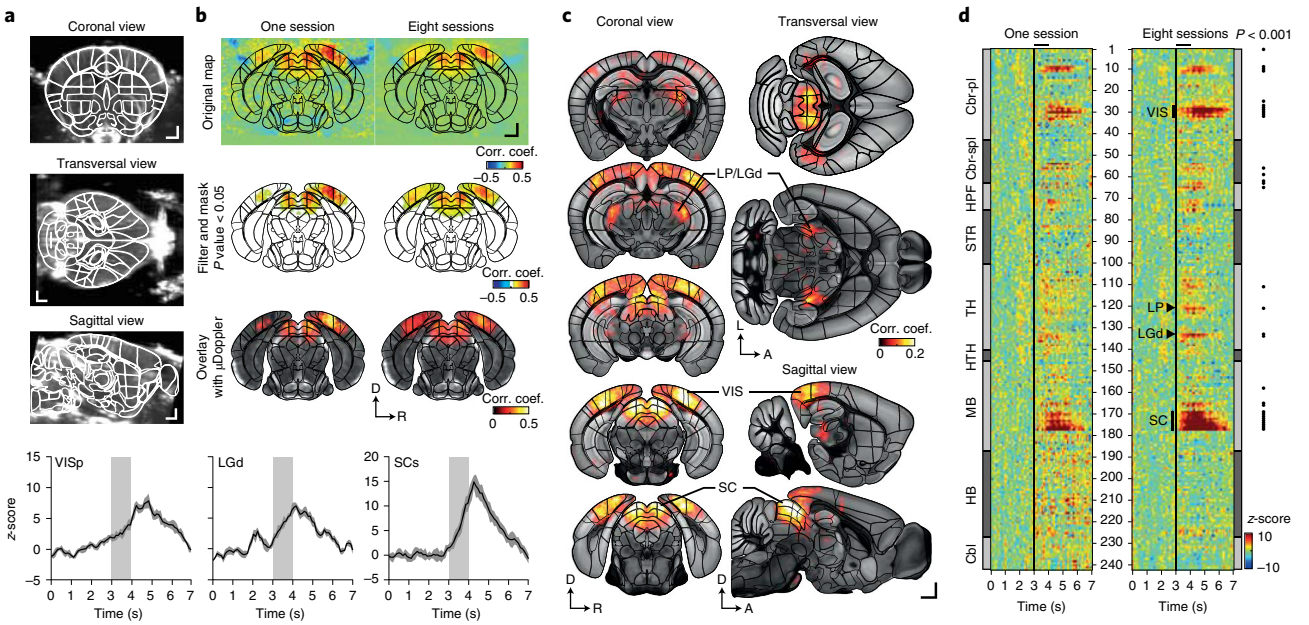

Fig. 6 | Example of processed whole-brain fUS data. a, Superimposition of registered coronal, transverse and sagittal anatomical views with regions of the Allen Mouse CCF, outlined in white (top to bottom; see Fig. 4a,b for registration software and landmarks for a correct alignment). **b**, Examples of visually evoked activity maps for one coronal brain slice (top to bottom: original, filtered, and overlaid with the µDoppler image) for single- and multisession average (respectively left and right columns). Regions from the Allen Mouse CCF are overlaid (black outlines). **c**, Coronal, transverse and sagittal activity maps from multiple sessions from the same mouse depicting only visually evoked activated voxels ($P < 0.05$, eight sessions) with segmented brain regions from the Allen Mouse CCF (black outlines). **d**, Left: region–time traces of 242 brain regions from single and multiple sessions from the same mouse. Right: activated brain regions with a P value < 0.001 (GLM followed by t-test across sessions). Brain regions are ordered by major anatomical structures and listed in Supplementary Table 1. Vertical line, stimulus start; horizontal line, stimulus end. **e**, Average response curves from the VISp, the lateral geniculate nuclei (LGd) and the SCs. Data are mean z-score ± standard error of the mean. The gray vertical bar represents the visual stimulus. A, anterior; L, left; R, right; D, dorsal. Scale bars, 1 mm. All animal experiments were approved and conducted according to the Committee on Animal Care of the Catholic University of Leuven, Belgium, the Veterinary Department of the Canton of Basel-Stadt, Switzerland, and European guidelines.

Reagent setup

Fentanyl/medetomidine/midazolam (FMM) solution

Mix 1 ml of fentanyl (0.05 mg/kg), 0.5 ml of medetomidine (0.5 mg/kg) and 1 ml of midazolam (5.0 mg/kg) with 7.5 ml distilled sterile water to a final concentration of 10 ml/kg. Inject 0.2 ml/20 g body weight. FMM solution can be stored at 4 °C for a couple of weeks. **! CAUTION** Listed drugs are controlled substances and must be used according to institutional and governmental guidelines.

Atipamezole/flumazenil/naloxone (AFN) solution

Mix 0.5 ml of atipamezole (1.25 mg/kg) 5 ml of flumazenil (0.25mg/kg) and 3 ml of naloxone (0.6 mg/kg) with 1.5 ml distilled sterile water to a final concentration of 10 ml/kg. Inject 0.2 ml/20 g body weight. AFN solution can be stored at 4 °C for a couple of weeks. **! CAUTION** Listed drugs are controlled substances and must be used according to institutional and governmental guidelines.

Ketamine/medetomidine solution (can be used as an alternative to FMM anesthesia)

Mix ketamine (100 mg/ml) with medetomidine (100 mg/ml) and 8 ml sterile saline, and inject 0.1 ml/20 g body weight intraperitoneally. Ketamine/medetomidine solution can be stored at 4 °C for a couple of weeks. **! CAUTION** Listed drugs are controlled substances and must be used according to institutional and governmental guidelines.

Glucose–saline solution

Mix glucose powder into saline to yield a 5% (wt/vol) solution. Vortex to dissolve glucose crystals. The solution can be stored at 4 °C for several weeks if sterility is preserved. For larger volumes, small aliquots can be frozen until needed. Defrost to room temperature (~20–23 °C) before use.

Superbond C&B

Follow the instructions of the user guide provided with the product: dispense one spoon of the polymer L-type radiopaque powder with four drops of monomer in the ceramic dish. Add one drop of catalyst V, and mix with an application brush. Extend the window of cement pliability by cooling down the ceramic tray with ice. Clean the ceramic dispensing dish with 70% ethanol before and after use. **! CAUTION** Resin cement is highly volatile and flammable. Avoid skin contact, and limit vapor inhalation. Careful handling is recommended.

Silicone rubber

In a sterile dish, dispense equal amounts of parts A and B (1:1 ratio), mix to homogenize and apply quickly with a spatula.

Equipment setup

Surgical instruments

Clean and sterilize surgical instruments and the headpost by autoclave or using a hot bead sterilizer before starting the surgery. Gel foam, cotton tip applicators and absorption spears must be autoclaved prior to the surgery. Clean surgical and imaging workspaces with 70% ethanol.

Ultrasound setup

Follow the instructions detailed in the miniScan manual (our demo acquisition GUI, see Fig. 3 and Supplementary Software) to install the hardware and software schematized in Fig. 3a. In brief, the fUS scanner is composed of four main parts: (i) the ultrasound transducer; (ii) the ultrasound electronics; (iii) the high-performance computing workstation and (iv) the software package. Additional components include a linear motor for moving the transducer and a second computer used here for managing visual stimulation.

This hardware–software configuration produces images of the brain vasculature with a resolution of 100 μm laterally (x), 110 μm in depth (z) and 300 μm in elevation (y), as previously measured[6] (Fig. 3c). The ultrasound sequence generated by the software is the same as that used in Macé et al.[6] and is detailed in Box 2.

The system has a default set of parameters optimized for imaging the mouse brain with the suggested hardware, as in the example presented here. The parameters can be modified through the file 'parameterUser.m' (see manual of the Supplementary Software). This file enables the settings of the system to be changed, including changing the probe, modifying the ultrasound sequence, changing spatial and temporal resolutions, customizing the trigger and randomizing the mechanical scanning of the brain slices. We strongly recommend starting with the default settings before making any modifications in the sequence.

Communication between the computers is via a serial port. When the acquisition GUI is launched, it automatically opens a serial port for that purpose. At each brain slice acquisition, a trigger is sent out to the external device (here the visual stimulation computer) to start the stimulus. The user can specify when the trigger should be sent with regard to the fUS acquisition in the parameter file ('parameterUser.m', see manual of the Supplementary Software). Moreover, another trigger can be sent through the BNC OUT port of the scanner at every ultrasound emission.

All imaging equipment, including the ultrasound probe and mouse holder, should be attached securely on an antivibration table. Equipment that may generate vibrations (fans or motors) must not be placed on the antivibration table. It is also recommended to ground this table to reduce electronic interference with the ultrasound probe.

Procedure

Animal preparation ● Timing ~3–4 h

! CAUTION Procedures involving live animals must be performed by trained experimenters and follow institutional guidelines, and local and national regulations.

▲ CRITICAL To ensure an efficient fUS imaging session under awake conditions, we recommend undertaking handling habituation by the experimenter for 5 days prior to surgery, as described in Box 1A.

▲ CRITICAL Inject the mouse with 5% (wt/vol) glucose solution (200 μl/25 g body weight)

Box 2 | Ultrasound sequence

The fUS sequence has six nested levels. The timeline of the sequence is shown in Fig. 3e. Here we describe in detail each step of the default sequence for advanced users.

Emission/reception block. A short ultrasound pulse of two wavelengths is sent out by all the elements of the probe with a specific delay to generate a tilted plane wave that propagates through the brain. Based on the speed of sound, the backscattered echoes recorded by the probe from 3.9 µs to 16.2 µs after emission correspond to depths between 3 mm and 11 mm. A dead time is included between emissions to ensure a fixed framerate of 500 Hz for the compound image.

Plane-wave block. A plane-wave acquisition block is obtained by repeating the emission/reception block three times and averaging the received signal to increase the signal-to-noise ratio.

Compound image. To increase the resolution of the image, seven tilted plane-wave blocks (−6° to 6° in steps of 2°) are acquired at a rate of 3.5 kHz. The echoes of the seven plane-wave blocks are beamformed to create seven plane-wave images and coherently added to generate a single compound image with high resolution (Fig. 3d, left)[5].

µDoppler image. The compound images are repeated continuously at a framerate of 500 Hz (Fig. 3d, left). Each set of 50 (fast mode) or 250 (slow mode) compound images is filtered to extract the blood signal (Fig. 3d, center) using a high-pass filter and an SVD filter[5]. Finally, the intensity of the filtered images is averaged to obtain a vascular (or µDoppler) image in 0.1 s/10 Hz (fast mode) or 0.5 s/2 Hz (slow mode) (Fig. 3d, right).

Trial. A trial consists of acquiring N µDoppler images at a specific brain slice. In our example data, 70 images are acquired in 7 s using the fast mode for each slice. A trigger is sent at the image N_i to the stimulation computer, here at image 35, starting the 1 s long visual stimulus (Fig. 3a).

Scan. To obtain a brain-wide functional scan, the probe is moved using the motor (Fig. 3a,b) by steps of 300 µm, and a new trial is performed at each position. The brain slices can be acquired in a sequential or randomized way. The full scan is obtained in ~2.5 min. Note that the recording time of a scan depends linearly on the number of slices and that a scan requires the stimulus to be repeated at each brain slice. Note also that ~300 µm between slices is optimal given the resolution of the ultrasound probe, and that oversampling will not increase the spatial resolution. Here six scans per session were acquired, leading to a recording time of ~15 min.
The software offers a fast mode that uses 50 compound images per µDoppler image (10 Hz) and a slow mode that uses 250 compound images (2 Hz) (Fig. 3b). Importantly, there is no change of signal-to-noise ratio between the two modes (averaging five frames from the fast mode is equivalent to one frame of the slow mode). The fast mode is better suited to measure responses to short stimulus or timing differences between regions, but produces a higher data volume than the slow mode.
The default settings of the sequence are optimized for the probes Vermon L15-Xtech (or Verasonics L22-14Vx) and for imaging the mouse brain. However, advanced users can set their sequence and adapt it for different configurations by changing the parameter file (see 'parameterUser.m'). In particular, the parameters can be changed to cover different frequencies ranges and penetration depths, the trigger can be customized and the acquisition of the brain slices can be randomized (see the manual in the Supplementary Software).

intraperitoneally to prevent dehydration during surgery. Give the first injection 2 h after the start of surgery, and repeat every 2 h.

1 Fill the induction chamber with 4% (wt/vol) isoflurane. Place the animal inside the induction chamber and wait ~3 min until the mouse becomes unconscious.
! CAUTION Isoflurane is an anesthetic gas with known adverse effects in humans and therefore must be handled in accordance with institutional guidelines. The use of isoflurane should be conducted in a designated area with appropriate ventilation and charcoal-based scavenging systems.

2 Inject FMM solution s.c. (0.2 ml/20 g body weight, see 'Reagent setup'), switch off isoflurane and move the mouse back to its cage while the drug takes full effect (~5 min). When the anesthesia is confirmed by lack of reflexes, transfer the mouse to the stereotaxic frame.
▲ CRITICAL STEP As an alternative to FMM anesthesia, you can instead inject ketamine/medetomidine solution i.p. (0.1 ml/20 g body weight).

3 Place the animal in a prone position on a heating pad set at 37.0 ± 0.5 °C, and fix the head in the stereotaxic frame. Adjust the animal's body such that the head is slightly elevated with respect to the trunk.
! CAUTION Under anesthesia, animals are unable to regulate their core temperature, potentially leading to hypothermia. The core body temperature should thus be maintained by use of a heat pad throughout anesthesia; check body temperature throughout using a rectal thermometer.
! CAUTION Excessive elevation may cause breathing problems. To prevent other breathing issues, pull the tongue out and to one side with dull forceps.

4 Test the depth of anesthesia by pinching the animal's toe; the anesthesia should be deep enough for this to elicit no response. When anesthesia is confirmed, administer i.p. injection of dexamethasone (0.5 mg/kg body weight), and wait 5 min for it to take effect. Lubricate both eyes with Duratears ointment to avoid dehydration.

5 Shave the top of the animal's head, then clean and wipe it with an iso-betadine solution using a sterile gel foam.

6 Make a midline incision with a scalpel blade from between the eyes to the back of the head. Expose the entire width of the skull by removing both the skin and the periosteum using fine straight scissors.

7 Under the stereomicroscope, insert closed angled forceps between the temporalis muscle and the skull a few millimeters anterior to the bregma. Run the angled forceps gently back to lambda.

8 Apply Vetbond tissue adhesive to the retracted muscles and the edges of the incision to secure the skin (Fig. 2a).

▲ **CRITICAL STEP** Avoid getting glue near the eyes, and be careful not to glue tissues (fur, skin or ears) to the stereotaxic frame.

▲ **CRITICAL STEP** Retraction of lateral muscles remains essential to assess lateral parts of the skull and enlarge the imaging field of view (Fig. 2i).

9 Dry the skull, and scrape it with the scalpel blade.

10 Adjust the headpost over the skull. Glue the headpost in the desired position using the tissue adhesive Vetbond. Wait 5 min to ensure good adhesion of the headpost to the skull before applying cement.

▲ **CRITICAL STEP** It is essential to prepare the skull well and glue the headpost firmly to ensure the headpost is stable after the cement is applied.

▲ **CRITICAL STEP** Make sure the headpost is parallel to the skull.

▲ **CRITICAL STEP** The design and position of the headpost determines how much of the brain can be imaged. This step may be adapted to optimize the field of view depending on the application.

11 Mix the cement as described in 'Reagent setup', and cement the headpost to the skull. Wait 10 min to ensure it is fixed firmly. Screw the headpost to the mouse holder, release and remove both the mouth clamp and ear bars of the stereotaxic frame.

▲ **CRITICAL STEP** Cool down the ceramic tray with ice to keep the cement pliable for longer.

! **CAUTION** Resin cement is highly volatile and flammable. Avoid skin contact, and limit vapor inhalation. Careful handling is recommended.

12 With a 0.05 mm burr, mark the surface of the skull by drilling very gently, to outline the shape and position of the window. Similarly, divide and mark the window into small 3 × 3 mm square plaques.

13 Drill skull plaques with a 0.05 mm burr by applying slight pressure to the skull with gentle movements.

! **CAUTION** To prevent drill-induced overheating of the brain tissue and clear bone debris, apply sterile saline frequently throughout the surgical procedure. However, always drill when the bone is dry as it is easier and more precise.

▲ **CRITICAL STEP** Due to skull stratification, the bone might bleed during the thinning process. Avoid long periods of bleeding.

? **TROUBLESHOOTING**

14 Keep drilling until a very thin and homogeneous preparation has been obtained (Fig. 2b). Apply sterile saline to make the bone more transparent: if no blood vessels can be seen through the thinned skull, repeat Steps 13–14 as necessary.

▲ **CRITICAL STEP** Note that well-performed thinning surgery substantially reduces the risk of tissue inflammation.

! **CAUTION** At this step, any mistake could break the thinned skull and damage the dura mater and the brain surface (Fig. 2i).

! **CAUTION** The sagittal suture should be treated with caution; any mistake could rupture the superior sagittal sinus and kill the animal by exsanguination.

? **TROUBLESHOOTING**

15 Crack the thinned skull at a corner of the window. Insert the angled forceps between the square of skull and the dura mater to dissociate them.

! **CAUTION** Do not puncture the dura mater. Do not let the dura mater dry.

16 Carefully remove one square of skull after the other in one hemisphere. Continuously clean and rinse the brain with sterile saline (Fig. 2c).

17 Continue to carefully remove the skull plaques from the second hemisphere (Fig. 2d). Delicately insert a 45°-angled forceps right under the skull, between the bone and the dura mater. Scratch carefully the bottom part of the skull to disconnect the dura mater from the bone. Proceed mm after mm, until the two tissues along the superior sagittal sinus have been completely disconnected.

▲ **CRITICAL STEP** The sagittal suture should be treated with caution as the superior sagittal sinus lies under it. Special care must be taken while crossing the bregma suture; the dura mater strongly connects with the bone and might be damaged if not disconnected carefully. If this procedure seems too risky, a thin band of bone can be left over the sinus. However, bear in mind that the remaining strip will result in attenuation of the signal in the medial part of the brain during the imaging sessions. Before continuing, we recommend waiting 10 min to ensure that no bleeding arises.

? **TROUBLESHOOTING**

18 Fill the window with 5 µl enrofloxacin solution (5 mg/kg), wait 10 min for it to take effect and then rinse with sterile saline.

19 Cut the plastic sheet with scissors to a size that fits the cranial window.

20 Carefully position the plastic sheet on the cranial window, and glue the edges to the bone.
! CAUTION Because of the curvature of the brain, it is possible for air to get trapped between the plastic sheet and the brain. If the plastic sheet is well sealed, these air pockets will fill with cerebrospinal fluid over the following days. The window should be fully transparent (no air gaps) at the time of imaging; thus it is important the sheet is well sealed.

21 Mix the cement as described in 'Reagent setup', and cement the plastic sheet to the bone. Wait 10 min to ensure the cement grips well (Fig. 2e).

22 Prepare the silicone rubber as described in 'Reagent setup', and quickly fill the window up with it. Wait 10 min until it hardens (Fig. 2f).

23 Inject AFN solution s.c. (0.2 ml/20 g body weight, see 'Reagent setup') to reverse the FMM anesthesia. If the alternative ketamine/medetomidine anesthesia has been used, inject atipamezole (1.0–2.5 mg/kg) to reverse the anesthesia. Inject the painkiller buprenorphine i.p. (0.05–0.1 mg/kg) and the antibiotic cefazolin (6.25 mg/kg). Add 1 ml of antibiotic emdotrim to 300 ml of drinking water.

24 Remove the rectal probe, and free the animal from head fixation.

25 Allow the mouse to recover from the anesthesia in its cage, placed on a heating pad, and observe regularly (Fig. 2g). Ease the mouse's recovery by providing dry food soaked in water and recovery gel to facilitate chewing and hydration.
■ PAUSE POINT We recommend at least 5 d of recovery before starting head-fixation habituation and imaging. During the first 3 d, we provide buprenorphine, dexamethasone and cefazolin and inject dexamethasone for an additional 2 d.

Imaging session ● Timing ~45 min

▲ CRITICAL To ensure an efficient fUS imaging session under awake conditions, we recommend undertaking head-fixation habituation prior to the imaging session for a minimum of 3 d, as described in Box 1B.

▲ CRITICAL Throughout the procedure, buttons of the acquisition GUI are indicated as [GUI panel/Button]. An image of the GUI is shown in Fig. 3f and Supplementary Software.

26 On the day of imaging, allow the animal to walk into the tube. Hold the headpost, and screw it to the mouse holder (Fig. 2h).
? TROUBLESHOOTING

27 Clean both the protective silicone rubber and the headpost with 70% ethanol using cotton tips. Rinse with sterile saline. Insert 1 mm of the 45°-angled forceps between the silicone rubber and the cement. Disconnect the silicone rubber from the cement all around the inner window of the headpost. Add a drop of sterile saline to smooth the disconnection of the silicone with the plastic window, and use fine forceps to catch and slowly remove the silicone plug from the headpost (Fig. 2h)
! CAUTION Take care while removing the silicone rubber not to remove the plastic sheet or damage the brain tissue.

28 Cover the imaging window with ultrasound gel (Fig. 2h).
! CAUTION Air bubbles trapped in the gel are echogenic and thus attenuate the signal (Fig. 2i). Load the ultrasound gel in a vial, and centrifuge (~500*g* for 2 min) before applying.

29 Place the animal under the ultrasound probe. Roughly adjust the ultrasound probe to the imaging window using the manual micromanipulator (Fig. 2h)
! CAUTION To avoid scratches on the probe and compressing the animal's brain, do not press the probe down against the headpost. The probe does not need to be in contact with the brain; ideally, place it ~3 mm above the surface.

30 In MATLAB, open the acquisition GUI ('start_miniScan.m', Fig. 3f) that enables recording of different types of images (Bmode, µDoppler and Functional in single plane or full brain volume). Set the file name and the communication ports with the motor [GUI panel: motor settings/Button: serial port] and with the stimulus computer [GUI panel: stimulus/Button: serial port]. Select the fast mode to acquire at 10 Hz; otherwise, images are acquired in slow mode at 2 Hz. A description of how to use this software can be found in the manual of the Supplementary Software. The default settings are optimized for this experimental example, but users can modify most of the parameters (probe, ultrasound sequence, trigger, random or sequential scanning, etc.) by modifying the 'parameterUser.m' file (see manual of the Supplementary Software).

! CAUTION To avoid damage to the probe, free the space around it while initiating the motor.

! CAUTION High emission power can damage the probe. Be aware that increasing the voltage or the duty cycle might damage the probe.

31 Switch on the button [GUI panel: single-plane/Button: Bmode] for real-time display of morphological images, and adjust the ultrasound probe with the manual micromanipulator to center the brain in the middle of the image.

32 Check the imaging quality using single plane μDoppler images with the button [GUI panel: single-plane/Button: Doppler] while moving along the cranial window using the button [GUI panel: motor settings/Button: move].

▲ CRITICAL STEP This step checks whether there is any brain damage caused by the cranial window implantation and whether any air bubbles or other artifacts are present that will degrade the image quality. Examples of such cases are shown in Fig. 2i.

? TROUBLESHOOTING

33 Move the ultrasound probe to the anterior edge of the cranial window to define the first plane of the scan.

! CAUTION For the sake of reproducibility over sessions, users are encouraged (i) to identify a brain slice that can easily and reproducibly be localized by the user using the single-plane μDoppler mode, (ii) to navigate to this slice at the beginning of the imaging session and (iii) to use this slice as a reliable origin. Then, the user should identify the coordinates of the anterior and posterior limits of the cranial window with respect to the origin using the single-plane μDoppler mode. These limits can be identified by a typical signal attenuation due to the presence of the skull (Fig. 2i). The registration step of the analysis will ensure a fine alignment of the scans across sessions, but following this procedure will avoid excessive shifts that could affect the extreme parts of the scan upon averaging, particularly when the number of slices is optimized to exactly span the cranial window size. Finally, note that the motor works in both directions. Be sure to identify the direction of the motor with regard to the mouse position. Here we assume that increasing values correspond to a movement of the probe from the anterior to the posterior part of the brain.

34 Run the anatomical scan [GUI panel: scan-volume/Button: Doppler] with a 100 μm step size between planes. The anatomical scan records a single μDoppler image at each position of the probe and saves the data as a single 3D matrix file. Example settings of the anatomical scan can be found in the manual of the Supplementary Software.

? TROUBLESHOOTING

35 Run the functional scan [GUI panel: scan-volume/Button: functional] with a 300 μm step size between planes (typically 20 planes). The functional scan acquires 70 μDoppler images at 10 Hz in fast mode (or 2 Hz when the fast mode button is unchecked) in each imaging plane and sends a trigger to start the stimulus (trigger sent at image 35). Data is saved as a single 4D matrix file (3D + time). Settings of the functional scan can be found in the manual of the Supplementary Software.

! CAUTION When using a new stimulation paradigm, for the first functional scan acquisition, check that the stimulation is correctly triggered before acquiring multiple scans.

? TROUBLESHOOTING

36 Acquire additional functional scans by repeating Step 35, or move to the next step to close the imaging session.

37 Move the ultrasound probe away from the mouse using the manual micromanipulator, wipe the gel away and clean the plastic window.

38 Prepare the silicone rubber as described in 'Reagent setup, and quickly fill the cranial window with it. Wait 10 min until hardened. Unscrew the headpost from the mouse holder, and put the animal back in its homecage. Cleaning and grooming behaviors are signs of good welfare.

■ PAUSE POINT Allow at least a 24-h rest period before the next imaging session.

Analysis of a single session ● Timing ~1 h/session

▲ CRITICAL In this section we provide a complete analysis package for data processing running with MATLAB including: (i) the registration of the fUS dataset with the Allen Mouse CCF reference atlas (Fig. 4a–c), (ii) the visualization of activity using correlation maps, (iii) the segmentation of the data into anatomical regions and (iv) the statistical procedure for coherent analysis of a single session or multiple sessions (Fig. 4d,e). Detailed documentation about files and functions used hereafter can be found in the manual of the Supplementary Software. The output of a single fUS session consists of one anatomical scan A (x,y,z) and a set of functional scans F_i (x,y,z,t), all used in the following analysis steps.

Registration with the reference brain atlas

39 Open the registration GUI ('registration_ccf.m') to register the anatomical scan $A(x,y,z)$ with the Allen Mouse CCF (see 'example01_registering.m').

40 Use the coronal view of the scan to center the volume on the atlas. Move the scan with the computer mouse (left-click for translation, right-click for rotation), and adjust the surface of the brain to the outline of the atlas. If needed, scale the (x,y,z) dimensions to fit the outlines of the atlas. The registration GUI is illustrated in Fig. 4a.

41 Rotate along the anteroposterior axis to align the superior sagittal sinus to the sagittal atlas outlines. If needed, rotate along the mediolateral axis to align the brain midline.
? TROUBLESHOOTING

42 Adjust the position of the brain scan to the atlas using brain landmarks, such as lateral ventricles, hippocampus and large vessels.

43 Repeat Steps 40–42 to ensure correct registration of the anatomical scan. An example of correct registration with landmarks is provided in Fig. 4b.

The output of the 'registration_ccf.m' function is an affine coordinate transformation:

$$\vec{r\prime} = M\vec{r} + \vec{a}$$

where $\vec{r} = (x, y, z)$ are the original coordinates of the anatomical scan, M is the rotation and scaling matrix and $\vec{a}$ the translation vector.

This affine transformation can be applied to any matrix having both the same voxel size as the Allen Mouse CCF (i.e., 50 μm^3 isotropic) and the same axis origin as the anatomical scan.
? TROUBLESHOOTING

Data stability and frame rejection

▲ CRITICAL These steps are important as they check the stability of the data and identify images affected by the movement artifacts (see 'example02_filter_average.m').

44 Run the function 'image_stability.m'. This function computes the average value of each frame, displays a histogram of the average values and fits it with a Gaussian curve (Fig. 5). Values higher than three times the standard deviation are considered as outliers due to movement artifacts. The position (plane and time) of the outliers is also displayed in a figure.
■ PAUSE POINT Three scenarios are possible. If there are few outliers (<10%) randomly distributed, the acquisition can be considered as 'stable' (Fig. 5, left). A high number of outliers (>10%) indicates a mechanical instability (Fig. 5, middle). In this case, check both the headpost and the animal fixation. If the outliers systematically happen around the stimulus time, it suggests that the artifact is generated by a behavioral movement related to the task, and this time period must be considered as a blind time as the data cannot be recovered through averaging (Fig. 5, right).
? TROUBLESHOOTING

45 Run the function 'image_rejection.m'. This function eliminates the outlier frames identified as in Step 44 and replaces them by an interpolation of the neighboring accepted frames.

Session average

46 Average all the motion-filtered scans from the same session (see 'example02_filter_average.m').

$$F_{aver}(x, y, z, t) = \frac{1}{N}\sum_{i=1}^{N} F_i(x, y, z, t)$$

These scans all share the same transformation matrix for registering.

Extract activity maps

47 This process enables visualization of the activated voxels. Follow option A to perform Pearson's correlation or option B to run a generalized linear model (GLM) analysis. Choose option A if you have a single type of stimulus (for example, here a flickering checkerboard presented for 1 s). Choose option B if you have multiple types of stimuli (for example, drifting gratings of different directions). Option B (GLM) is a more flexible method of generating activity maps as it can be extended to multiple stimuli or events by using multiple regressors. Note that option B also works in the case of one stimulus type, in which case it gives the same result as option A.

(A) **Pearson's correlation**.

(i) Run the function 'map_correlation.m' (see 'example03_correlation.m') to compute the correlation of the session dataset with the stimulus. This function defines the stimulus

pattern $s(t)$ as the correlation of the stimulation window $w(t)$ by the hemodynamic response $hrf(t)$,

$$s(t) = w(t) * hrf(t),$$

normalizes the data and the stimulus with zero-means

$$\overline{F}_{aver}(x,y,z,t) = F_{aver}(x,y,z,t) - \frac{1}{n}\sum_{i=1}^{n} F_{aver}(x,y,z,t),$$

$$\overline{s}(t) = s(t) - \frac{1}{n}\sum_{i=1}^{n} s(t),$$

computes the Pearson's correlation in each voxel of the image. The output of the function is a volumetric correlation map:

$$c(x,y,z) = \frac{\sum_{i=1}^{n} \overline{F}_{aver}(x,y,z,t)\overline{s}(t)}{\sqrt{\sum_{i=1}^{n} \overline{F}^2_{aver}(x,y,z,t)\sum_{i=1}^{n} \overline{s}^2(t)}}.$$

A default model of the hrf is provided in the script (based on the hrf from the SPM software[46]). Voxels with $c > 0.23$ are considered as significantly activated for this example. This threshold is defined by selecting a P-value threshold of 0.05, converting the P-value threshold into the corresponding z-score using a two-tailed t-test ($z = 2.8$), and computing a z-score value from the correlation using Fisher's transform $z = \sqrt{n-3}Arctanh(c)$, with n being the number of samples. For $n = 70$ and $z = 2.8$, the threshold is $c = 0.23$.

(B) **Run a GLM**.

(i) Run the function 'map_glm.m' (see 'example04_glm'). This function defines a model with two regressors

$$y(t) = \beta_1 X_1(t) + \beta_2 X_2(t),$$

where the first regressor is the stimulus convolved with the hemodynamic response

$$X_1(t) = w(t) * hrf(t),$$

and the second regressor is a constant $X_2(t) = 1$.

The function fits each voxel of the averaged scan $F_{aver}(x,y,z,t)$ with this model using the Matlab function glmfit (no regularization step used). The output is a set of estimators for each voxel $\beta_1(x,y,z)$, $\beta_2(x,y,z)$ and the t-score map corresponding to each estimator. The standard outputs of the GLM can be used for visualization of activity and contrasts between stimuli, and for statistical analysis at the subject or group level.

48 Register the activity map with the Allen Mouse CCF by running the function 'register_data.m'. This function interpolates anisotropic voxels of the scan (100 × 110 × 300 μm) to isotropic voxels of the Allen Mouse CCF (50 × 50 × 50 μm) to generate a 3D matrix $c_{int}(x,y,z)$ and transforms the interpolated data into the register coordinates $C(\vec{r}\prime) = c_{int}(\vec{r})$, where $\vec{r} = M^{-1}(\vec{r}\prime - \vec{a})$. The registered data can be displayed with the anatomical outlines (see 'draw_borders.m').

Analysis of region-time traces

▲ **CRITICAL** This analysis enables temporal activity to be analyzed in each anatomical region defined by the Allen Mouse CCF (see 'example05_segmentation.m').

49 Run 'segmentation_ccf.m' to segment the averaged scan. This function interpolates the functional data from a voxel size of 48 × 100 × 300 μm to an isotropic voxel size of 50 × 50 × 50 μm. The data are resampled to the same voxel size as the reference atlas to make them compatible with the registration procedure of Steps 39–43. Then, the function registers the interpolated data using the affine transformation matrix obtained after Step 43. The functional data is interpolated and registered as follows:

$$F_{int}(x,y,z,t) = interpolate(F_{Aver}),$$

$$F_{reg}(\vec{r},t) = F_{int}\left(M^{-1}(\vec{r} - \vec{a}), t\right).$$

All voxels from the same region are then integrated as follows:

$$S(k,t) = \sum_{\vec{r} \in region\ k} F_{reg}(\vec{r},t)$$

50 Run the function 'select_brain_regions.m' to extract a selection of brain regions. Generate a region–time matrix $z(k,t)$, normalized as a z-score with zero average and standard deviation 1 in the baseline,

$$z(k,t) = \frac{S(k,t) - \overline{S}(k)}{\sqrt{\sum_{t=1}^{n} \left(S(k,t) - \overline{S}(k)\right)^2}},$$

with $\overline{S}(k) = \frac{1}{n}\sum_{t=1}^{n} S(k,t)$ and n being the number of samples in the baseline.

Analysis of multiple sessions ● Timing ~1 h

▲ CRITICAL This section focuses on the analysis of multiple sessions from a single mouse. This section should be followed after each session i has already been through Steps 39–50, and both the activity map $C_i(x,y,z)$ and a region–time matrix $z_i(k,t)$ have been extracted. This analysis aims to obtain a statistical view of what is significantly activated over multiple imaging sessions.

Activity maps

▲ CRITICAL The activity maps $C_i(x,y,z)$ from each session i are extracted after running Steps 39–47 of the **Procedure**. We used the activity maps based on correlation in this procedure, but it can be conceptually applied in the same way to activity maps (t-score maps) extracted using the GLM.

51 Run the function 'map_statistics' (see 'example06_multisession_map.m') to compute the mean value C_{mean}, the standard deviation σ and the t-score t_{score} of C_i in each voxel

$$C_{mean}(x,y,z) = \frac{1}{N}\sum_{i=1}^{N} C_i(x,y,z),$$

$$\sigma^2(x,y,z) = \frac{1}{N}\sum_{i=1}^{N} \left(C_i(x,y,z) - C_{mean}(x,y,z)\right)^2,$$

$$t_{score}(x,y,z) = \frac{C_{mean}(x,y,z)}{\sigma(x,y,z)}.$$

Then, compute the P value with a Student's distribution

$$p(x,y,z) = 1 - tcdf\left(t_{score}(x,y,z), N\right),$$

where $tcdf$ is the cumulative distribution function of the Student's t distribution. For a low number N, a pixel is considered significantly activated if $P < 0.05$. For larger numbers, one should apply a post hoc multiple comparison of the P value (e.g., Bonferroni, false discovery rate) to avoid false positives.

52 Display the significantly activated voxels of the averaged activity map with the anatomical outlines (see 'draw_borders.m').

Analysis of region–time traces

▲ CRITICAL The region–time matrices $z_i(k,t)$ from each session i are extracted after running Steps 48–50 of the **Procedure**.

53 Run the function 'segmentation_statistics.m' to perform a statistical study over all the sessions (see 'example07_multisession_segmentation.m'). This function computes the mean value

$$z_{mean}(k,t) = \frac{1}{\sqrt{N}}\sum_{i=1}^{N} z_i(k,t).$$

The division by $\sqrt{N}$ keeps the z_{mean} normalized with standard deviation equal to 1 in the baseline as in Step 47(B).

54 Define a significantly activated region by studying the correlation with the stimulus as in Step 47 (A) by:
generating the stimulus pattern $stim(t)$ as the correlation of the stimulation window $w(t)$ by the hemodynamic response $hrf(t)$

$$s(t) = w(t) * hrf(t),$$

subtracting the mean

$$\bar{s}(t) = s(t) - \frac{1}{n}\sum_{t=1}^{n} s(t),$$

computing the correlation in each region k and each session i,

$$r_i(k) = \frac{\sum_{t=1}^{n} z_i(k,t)\bar{s}(t)}{\sum_{t=1}^{n} z_i^2(k,t)\sum_{t=1}^{n}\bar{s}^2(t)},$$

computing the mean value, the standard deviation and the t-score of $r_i(k)$,

$$r_{mean}(k) = \frac{1}{N}\sum_{i=1}^{N} r_i(k),$$

$$\sigma^2(k) = \frac{1}{N}\sum_{i=1}^{N} (r_i(k) - r_{mean}(k))^2,$$

$$t_{score}(k) = \frac{r_{mean}(k)}{\sigma(k)},$$

and computing the P value with a Student's distribution

$$p(k) = 1 - tcdf(t_{score}(k), N),$$

where *tcdf* is the cumulative distribution function of the Student's t distribution.

55 Display the averaged region–time matrix $z_{mean}(k,t)$ with the significantly activated regions with $p(k) < 0.001$.

Troubleshooting

Troubleshooting advice can be found in Table 1.

Table 1 | Troubleshooting table

Step	Problem	Possible reason	Solution
13	Skull bleeding	A blood vessel was hit in the skull	Rinse with sterile saline and soak up blood with foam; in most cases, bleeding will stop. Apply bone wax if bleeding persists (see 'Reagents')
14	Drill burr breaches skull	Pressure applied was too strong	If brain tissue is not damaged and no bleeding arises from under the skull, keep drilling while reducing the strength. If brain tissue is damaged, terminate the surgery. Refine your motor skills for future surgeries. See Fig. 2i for an example of the impact of cortical damages on the μDoppler image quality
17	Sinus bleeding	Tweezer or skull bone breached the sinus. The dura covering the sinus was not correctly dissociated from the skull and was disrupted while removing the skull plaque	If the sinus breach is small, intensively pour saline and absorb the blood arising from the sinus with sterile gel foam. Maintain a light pressure on the slit for 5 min to contain the bleeding. If the bleeding stops, continue the procedure carefully, bearing in mind there is a high risk of reopening. Inject the appropriate volume of glucose solution (see 'Reagent setup') to balance the loss of blood. If the breach is too large, the bleeding cannot be stopped or the sinus is too damaged to be saved, terminate the surgery. Refine your motor skills for future surgeries
26	Removal of the headpost	Inadequate headpost fixation to the mouse skull bone	The headpost has been removed while the mouse was in its home cage: no solution; ensure the headpost is more securely fixed in future surgeries. Terminate the experiment
			The headpost has been removed during fixation, and the brain has been damaged: no solution; ensure the headpost is more securely fixed in future surgeries. Terminate the experiment

Table continued

Table 1 (continued)

Step	Problem	Possible reason	Solution
			The headpost has been removed during fixation, but no brain damage/bleeding occurred: anesthetize (Steps 1–4), and implant a new headpost more securely (Steps 9–11 and 18–25)
32	Signal artifacts (examples of results seen as a consequence of the following reasons are shown in Fig. 2i)	Narrow cranial window	No solution. Enlarge the cranial window in future surgeries
		Cortical bulge	No solution. Refine your motor skills, and be more delicate at dissociating skull plaques from the dura. Terminate the experiment
		Cortical damage	No solution. Refine your motor skills, and be more delicate at dissociating skull plaques from the dura. Terminate the experiment
		Air bubble trapped in the ultrasound gel	Remove the ultrasound gel carefully, and reapply, avoiding formation of air bubbles. Air bubbles can be removed from the gel by prior gel centrifugation
		Signal saturation from skull	Adjust gain, and/or smoothly move the probe away from this plane
34	Motor moves away from limits	User forgot to hit 'Set Origin' in the 'Motor settings' section of the GUI	Immediately hit the 'STOP' button in the *Motor settings* of the GUI. Manually reposition the motor over the window, and hit 'Set Origin'
35	Motion artifact during imaging session	Loose fixation of the headpost and/or the mouse holder	Control and reinforce the headpost and/or mouse holder fixation
		Light headpost-to-skull fixation	Control the headpost sealing, and reinforce the fixation to the skull following Steps 9–11 of the Procedure
		Excessive movement of the mouse in the tube	Reduce mouse stress and head-fixation habituation by reinforcing training stages. Follow recommendations provided in Box 1
41	Anterior planes are located at posterior position	Scan has been performed from posterior to anterior position	For the acquired dataset, flip the antero-posterior order in the both ScanAnat and ScanFus files. For future experiments, scan the brain from anterior to posterior position
43	Mistransformation of the dataset	Human error; the volume scan was not transformed appropriately	Repeat the transformation process, following tips and tricks shown in Fig. 4a,b
44	Frame rejection >10%	Loose fixation of the headpost and/or the mouse holder	Control and reinforce the headpost and/or mouse holder fixation
		Light headpost-to-skull fixation	Control the headpost sealing, and reinforce the fixation to the skull following Steps 9–11 of the Procedure
		Excessive movement of the mouse in the tube	Reduce mouse stress and head-fixation habituation by reinforcing training stages. Follow recommendations provided in Box 1

Timing

New fUS users should allow extra time to set up and troubleshoot their system installation, and thus ensure a fully working system before beginning experiments. The surgical time will decrease substantially with practice.

Steps 1–25, animal preparation: ~3–4 h
Steps 26–38, imaging session: ~45 min
Steps 39–50, analysis of a single session: ~1 h
Steps 51–55, analysis of multiple sessions: ~1 h
Box 1A, presurgery mouse handling: ~20 min
Box 1B, postsurgery head-fixation habituation: ~1 h

Anticipated results

This protocol describes how to insert cranial windows for fUS that are stable for several months (Steps 1–25). A brain-wide view of stimulus-evoked activity in an awake head-fixed mouse can subsequently be obtained in a short ~15 min imaging session. Outputs are standardized as brain-wide activity maps and activity traces in ~250 brain regions: these are suitable for statistical comparison over multiple sessions, and thus significance at the subject level can be inferred using the analysis software.

As an example, we imaged the brain network activated by a short visual stimulus of 1 s. The visual stimulus consisted of square checkerboards (10° spatial frequency) flickering at 5 Hz presented on a large screen directly in front of the mouse. We repeated six functional scans per imaging session (~2 min per scan), and we accumulated eight imaging sessions from the same mouse. By processing a

single session (Steps 39–50), the six functional scans acquired in that session (in ~15 min) were averaged, and the resulting activity map (Step 47; Fig. 6b, left) showed some significantly activated voxels. Single-session images are variable owing to the animal's ongoing behavior, and results from individual sessions must therefore be interpreted with caution. As an example, in the results averaged for Fig. 6b, we observed an asymmetry in the visual response although the stimulus was presented to both eyes.

An important advantage of this protocol is that data from different sessions can be combined, as they are registered and analyzed in a standardized way (Steps 51–55). Two types of output are extracted for each session: one activity map and one region–time matrix (Figs. 4 and 6). The Supplementary Software can be used to combine the activity maps and region–time matrices of multiple sessions to obtain one average map/time-region matrix per animal (Steps 51–55, Fig. 6).

On the activity map, by averaging the eight sessions from the same mouse (Fig. 6b, right) and choosing a threshold of $P < 0.05$ uncorrected, we observed a significant activation in the superior colliculus (SC), visual cortex (VIS), dorsal lateral geniculate complex (LGd) and other thalamic regions that are known regions of the mouse visual system. We also observed that the response became symmetric in the VIS and that fewer false-positive voxels are visible outside the brain. The software enables these whole-brain maps to be displayed in 3D by selecting different views, superimposed on the atlas to facilitate localizing the active voxels (Fig. 6c).

The region–time analysis gives a global view of the activity with a dynamic aspect (Fig. 6d). In the single session (Steps 49–50, Fig. 6d left), we visualized responses (i.e., high z-scores) after the presentation of the stimulus, for example in the SC and VIS. When the eight sessions were averaged (Steps 53–55, Fig. 6d right), we confirmed that these regions are significantly activated ($P < 0.001$ uncorrected), and we observed that more regions show significant activity than is visible in an individual session. The region–time analysis brings information about the dynamics of the response in different regions. In particular, we can see that activity peaks later in the primary visual cortex (VISp) compared with the SC and LGd, which is consistent with the fact that the SC and LGd receive direct retinal inputs whereas the VISp gets visual inputs indirectly. This qualitative observation is confirmed when inspecting the activity curves in these specific regions (Fig. 6e, VISp response peaks ~1 s later than in the SC and LGd).

The activity maps and the region–time representations provide complementary interpretation of the fUS data. While the activity map displays full spatial information, it is based on a priori knowledge of the hemodynamic response function, and ignores temporal differences between different regions. On the other hand, the region–time view keeps the temporal dynamics at the cost of losing some spatial information. For example, a small part of a region can be significantly activated and spatially detected but diluted and thus underestimated when averaged with inactivated voxels from the same region. The fact that regions have different sizes, unlike the voxel-based analysis, should also raise caution when interpreting the results.

As for other imaging modalities, individual sessions may give variable results. This variability can be largely explained by the spontaneous ongoing behavior and/or brain state of the mice. Indeed, it was observed using cortex-wide imaging methods that spontaneous behavior explains most of the variance in neuronal activity even in the presence of a stimulus or task[50,51]. We propose here a simple analysis method, but more advanced regression methods, which take into account the behavior variables, could be implemented by the users to refine the activity maps.

We believe that this comprehensive protocol will support implementation of the fUS technology to the neuroscience community. Getting access to brain-wide activity during behavior will hopefully contribute to better understanding brain functions at the network level.

Data availability

The example dataset is available on Zenodo[45] and can be downloaded at https://doi.org/10.5281/zenodo.4382638.

Code availability

All the codes used for data acquisition and for data analysis referenced in this protocol are provided as Supplementary Software. A copy is also available on a GitHub/Zenodo repository, along with potential updates[44] and can be downloaded at https://github.com/nerf-common/whole-brain-fUS.

References

1. Luo, L., Callaway, E. M. & Svoboda, K. Genetic dissection of neural circuits. *Neuron* **57**, 634–660 (2008).
2. Lerner, T. N., Ye, L. & Deisseroth, K. Communication in neural circuits: tools, opportunities, and challenges. *Cell* **164**, 1136–1150 (2016).
3. Hong, G. & Lieber, C. M. Novel electrode technologies for neural recordings. *Nat. Rev. Neurosci.* **20**, 330–345 (2019).
4. Mace, E. et al. Functional ultrasound imaging of the brain. *Nat. Methods* **8**, 662–664 (2011).
5. Mace, E. et al. Functional ultrasound imaging of the brain: theory and basic principles. *IEEE Trans. Ultrason. Ferroelectr. Freq. Control* **60**, 492–506 (2013).
6. Macé, É. et al. Whole-brain functional ultrasound imaging reveals brain modules for visuomotor integration. *Neuron* **100**, 1241–1251.e7 (2018).
7. Urban, A. et al. Chronic assessment of cerebral hemodynamics during rat forepaw electrical stimulation using functional ultrasound imaging. *Neuroimage* **101**, 138–149 (2014).
8. Urban, A. et al. Real-time imaging of brain activity in freely moving rats using functional ultrasound. *Nat. Methods* **12**, 873–878 (2015).
9. Brunner, C. et al. Evidence from functional ultrasound imaging of enhanced contralesional microvascular response to somatosensory stimulation in acute middle cerebral artery occlusion/reperfusion in rats: a marker of ultra-early network reorganization? *J. Cereb. Blood Flow Metab.* **38**, 1690–1700 (2018).
10. Brunner, C. et al. Mapping the dynamics of brain perfusion using functional ultrasound in a rat model of transient middle cerebral artery occlusion. *J. Cereb. Blood Flow Metab.* **37**, 263–276 (2017).
11. Rau, R. et al. 3D functional ultrasound imaging of pigeons. *Neuroimage* **183**, 469–477 (2018).
12. Demené, C. et al. Multi-parametric functional ultrasound imaging of cerebral hemodynamics in a cardio-pulmonary resuscitation model. *Sci. Rep.* https://doi.org/10.1038/s41598-018-34307-9 (2018).
13. Bimbard, C. et al. Multi-scale mapping along the auditory hierarchy using high-resolution functional ultrasound in the awake ferret. *eLife* https://doi.org/10.7554/eLife.35028 (2018).
14. Dizeux, A. et al. Functional ultrasound imaging of the brain reveals propagation of task-related brain activity in behaving primates. *Nat. Commun.* https://doi.org/10.1038/s41467-019-09349-w (2019).
15. Blaize, K. et al. Functional ultrasound imaging of deep visual cortex in awake nonhuman primates. *Proc. Natl Acad. Sci. USA* https://doi.org/10.1073/pnas.1916787117 (2020).
16. Imbault, M., Chauvet, D., Gennisson, J.-L., Capelle, L. & Tanter, M. Intraoperative functional ultrasound imaging of human brain activity. *Sci. Rep.* **7**, 7304 (2017).
17. Soloukey, S. et al. Functional ultrasound (fUS) during awake brain surgery: the clinical potential of intra-operative functional and vascular brain mapping. *Front. Neurosci*. https://doi.org/10.3389/fnins.2019.01384 (2020).
18. Demene, C. et al. Functional ultrasound imaging of brain activity in human newborns. *Sci. Transl. Med.* **9**, eaah6756 (2017).
19. Sieu, L.-A. et al. EEG and functional ultrasound imaging in mobile rats. *Nat. Methods* **12**, 831–834 (2015).
20. Rabut, C. et al. 4D functional ultrasound imaging of whole-brain activity in rodents. *Nat. Methods* **16**, 994–997 (2019).
21. Brunner, C. et al. A platform for brain-wide volumetric functional ultrasound imaging and analysis of circuit dynamics in awake mice. *Neuron* https://doi.org/10.1016/j.neuron.2020.09.020 (2020).
22. Rahal, L. et al. Ultrafast ultrasound imaging pattern analysis reveals distinctive dynamic brain states and potent sub-network alterations in arthritic animals. *Sci. Rep.* **10**, 10485 (2020).
23. Sans-Dublanc, A. et al. Optogenetic fUSI for brain-wide mapping of neural activity mediating collicular-dependent behaviors. *Neuron* https://doi.org/10.1016/j.neuron.2021.04.008 (2021).
24. Heo, C. et al. A soft, transparent, freely accessible cranial window for chronic imaging and electrophysiology. *Sci. Rep*. https://doi.org/10.1038/srep27818 (2016).
25. Ghanbari, L. et al. Cortex-wide neural interfacing via transparent polymer skulls. *Nat. Commun*. https://doi.org/10.1038/s41467-019-09488-0 (2019).
26. Rynes, M. L. et al. Assembly and operation of an open-source, computer numerical controlled (CNC) robot for performing cranial microsurgical procedures. *Nat. Protoc.* **15**, 1992–2023 (2020).
27. Kılıç, K. et al. Chronic imaging of mouse brain: from optical systems to functional ultrasound. *Curr. Protoc. Neurosci.* https://doi.org/10.1002/cpns.98 (2020).
28. Boido, D. et al. Mesoscopic and microscopic imaging of sensory responses in the same animal. *Nat. Commun.* https://doi.org/10.1038/s41467-019-09082-4 (2019).
29. Aydin, A. K. et al. Transfer functions linking neural calcium to single voxel functional ultrasound signal. *Nat. Commun.* https://doi.org/10.1038/s41467-020-16774-9 (2020).
30. Fonseca, M. S., Bergomi, M. G., Mainen, Z. F. & Shemesh, N. Functional MRI of large scale activity in behaving mice. Preprint at *bioRxiv* https://doi.org/10.1101/2020.04.16.044941 (2020).
31. Dinh, T. N. A., Jung, W. B., Shim, H.-J. & Kim, S.-G. Characteristics of fMRI responses to visual stimulation in anesthetized vs. awake mice. *Neuroimage* https://doi.org/10.1016/j.neuroimage.2020.117542 (2021).
32. Weisenburger, S. & Vaziri, A. A guide to emerging technologies for large-scale and whole-brain optical imaging of neuronal activity. *Annu. Rev. Neurosci.* **41**, 431–452 (2018).

33. Jun, J. J. et al. Fully integrated silicon probes for high-density recording of neural activity. *Nature* **551**, 232–236 (2017).
34. Steinmetz, N. A., Zatka-Haas, P., Carandini, M. & Harris, K. D. Distributed coding of choice, action and engagement across the mouse brain. *Nature* **576**, 266–273 (2019).
35. Sych, Y., Chernysheva, M., Sumanovski, L. T. & Helmchen, F. High-density multi-fiber photometry for studying large-scale brain circuit dynamics. *Nat. Methods* **16**, 553–560 (2019).
36. Lake, E. M. R. et al. Simultaneous cortex-wide fluorescence Ca2+ imaging and whole-brain fMRI. *Nat. Methods* **17**, 1262–1271 (2020).
37. Gottschalk, S. et al. Rapid volumetric optoacoustic imaging of neural dynamics across the mouse brain. *Nat. Biomed. Eng.* **3**, 392–401 (2019).
38. Demené, C. et al. Spatiotemporal clutter filtering of ultrafast ultrasound data highly increases Doppler and fUltrasound sensitivity. *IEEE Trans. Med. Imaging* **34**, 2271–2285 (2015).
39. Goldey, G. J. et al. Removable cranial windows for long-term imaging in awake mice. *Nat. Protoc.* **9**, 2515–2538 (2014).
40. Hillman, E. M. C. Coupling mechanism and significance of the BOLD signal: a status report. *Annu. Rev. Neurosci.* https://doi.org/10.1146/annurev-neuro-071013-014111 (2014).
41. Avants, B. B. et al. A reproducible evaluation of ANTs similarity metric performance in brain image registration. *Neuroimage* https://doi.org/10.1016/j.neuroimage.2010.09.025 (2011).
42. Pallast, N. et al. Processing pipeline for atlas-based imaging data analysis of structural and functional mouse brain MRI (AIDAmri). *Front. Neuroinform.* https://doi.org/10.3389/fninf.2019.00042 (2019).
43. Wang, Q. et al. The Allen Mouse Brain Common Coordinate Framework: a 3D reference atlas. *Cell* https://doi.org/10.1016/j.cell.2020.04.007 (2020).
44. ClemBrunner & nerf-common. nerf-common/whole-brain-fUS: whole-brain-fUS v1.0. Zenodo https://doi.org/10.5281/zenodo.4585348 (2021).
45. Mace, E. & Montaldo, G. Whole-brain visually evoked activity maps in head-fixed awake mice. Zenodo https://doi.org/10.5281/ZENODO.4382638 (2020).
46. Friston, K. J. et al. Statistical parametric maps in functional imaging: a general linear approach. *Hum. Brain Mapp.* **2**, 189–210 (1994).
47. Gouveia, K. & Hurst, J. L. Optimising reliability of mouse performance in behavioural testing: the major role of non-aversive handling. *Sci. Rep.* https://doi.org/10.1038/srep44999 (2017).
48. Hurst, J. L. & West, R. S. Taming anxiety in laboratory mice. *Nat. Methods* **7**, 825–826 (2010).
49. Guo, Z. V. et al. Procedures for behavioral experiments in head-fixed mice. *PLoS ONE* **9**, e88678 (2014).
50. Musall, S., Kaufman, M. T., Juavinett, A. L., Gluf, S. & Churchland, A. K. Single-trial neural dynamics are dominated by richly varied movements. *Nat. Neurosci.* **22**, 1677–1686 (2019).
51. Stringer, C. et al. Spontaneous behaviors drive multidimensional, brainwide activity. *Science* **364**, eaav7893 (2019).

Acknowledgements

We acknowledge the following grants to G.M. and A.U.: the Leducq Foundation (15CVD02), FWO (MEDI- RESCU2-AKUL/17/049, G091719N, and 1197818N), VIB TechWatch (fUSI-MICE), internal NERF TechDev fund (3D-fUSI project). We acknowledge the following grant to E.M.: Human Frontier Science Program Postdoctoral Fellowship (LT000769/ 2015) and the support of this work by the Max Planck Society. We acknowledge the following grant to B.R.: Swiss National Science Foundation grants (3100330B_163457), the National Center of Competence in Research Molecular Systems Engineering grant, European Research Council (669157, RETMUS), and DARPA (HR0011-17- C-0038, Cortical Sight). We thank M. Krumin for assistance with the design of the mouse holder, D. Kil for assistance with the design of the headpost and mouse holder, T. Lambert for help with the PsychoPi software, and A. Savoye and J. Tantivit for technical help at the beginning of the project. We also thank NERF animal caretakers I. Eyckmans, F. Ooms and S. Luijten for their help with the management of the mice.

Author contributions

E.M., B.R., G.M. and A.U. designed the project. E.M., G.M. and A.U. designed, assembled and tested the fUS system. E.M., C.B., M.G. and G.M. performed experiments. E.M. and G.M. designed and performed the data analysis. G.M. developed the software included with the manuscript. C.B., E.M., M.G., G.M, B.R. and A.U. wrote the manuscript.

Competing interests

A.U. is the founder and a shareholder of AUTC company commercializing neuroimaging solutions for preclinical and clinical research.

Additional information

Supplementary information The online version contains supplementary material available at https://doi.org/10.1038/s41596-021-00548-8.

Correspondence and requests for materials should be addressed to G.M. or E.M.

Peer review information *Nature Protocols* thanks Anne Churchland, Pablo Blinder, Yves Boubenec and the other, anonymous reviewer(s) for their contribution to the peer review of this work.

Reprints and permissions information is available at www.nature.com/reprints.

Publisher's note Springer Nature remains neutral with regard to jurisdictional claims in published maps and institutional affiliations.

Received: 23 September 2020; Accepted: 30 March 2021;
Published online: 04 June 2021

Related links
Key references that demonstrate the development and use of the protocol
Macé, É. et al. *Neuron* **100**, 1241–1251.e7 (2018): https://doi.org/10.1016/j.neuron.2018.11.031
Sans-Dublanc, A. et al. *Neuron* (2021): https://doi.org/10.1016/j.neuron.2021.04.008